Event Display: Can We See What We Want to See?[1]

H.Drevermann *CERN, Geneva*
D.Kuhn *Institut für Experimentalphysik der Universität Innsbruck*[2]
B.S.Nilsson *CERN, Geneva*, and *Niels Bohr Institute, Copenhagen*

Abstract

Due to the complexity of HEP detectors and their data the graphical representation of events is necessary, but also very demanding. The paper covers physiological aspects, e.g. choice of colours, human pattern recognition and 3D vision. For the unbiased understanding of the data realistic 2D and 3D projections, schematic projections and abstract 2D and 3D projections are discussed.

1 Introduction

High energy physics experiments investigate reactions between colliding elementary particles. To this purpose data on the particles leaving the collision point are recorded in large detectors and stored in digital form. The set of data recorded per collision is called an event. Practically all subdetectors are sampling devices, which for each event record the tracks of charged particles as a sequence of points, called hits, or record the showers of particles as a set of cells, for which the energy deposited is recorded as well.

The events are the basic units for further investigations, which are done by powerful pattern recognition and analysis programs. For checking of these methods and for presentation, the display of single events is an efficient tool, as visual representation is the most efficient way to transfer data from a computer to the human brain.

However, complexity of both events and detectors has increased substantially and will increase further. Higher event multiplicities and higher momenta of outgoing particles can be matched by more sophisticated detectors, i.e. detectors with a growing number of subunits of increasing granularity, resolution and precision. As a consequence pictures of detectors and events are getting more and more complicated and, in the extreme, may even get incomprehensible. The enormous improvements of detectors, of computers and of visual devices seems not to be matched by the “perception techniques” of the human eye and the human brain, as these have been developed long time ago for other objects than pictures of events. This leads to the question: Is a fast, efficient and unambiguous transfer of data to the human brain via visual techniques still possible for complicated events or will it be more convenient to read and interpret numbers?

Conventional graphics tries to represent events in the most realistic way[3]. However, it will turn out for a variety of applications, that these conventional representations result in pictures, which are not sufficiently clear. Therefore new visual representations are proposed here, which can better be tuned to the capabilities of human perception.

---

[1] This in an extended version of "Is there a Future for Event Display?” [1]
[2] Supported by grant of Fonds zur Förderung der Wissenschaftlichen Forschung, Austria
[3] Complicated events might be cleaned by selective presentation of parts of the data and the detector

For the use of graphical representations in talks and papers it is necessary to find pictures, which can be understood intuitively without omitting relevant information. For this purpose in this article we will discuss:

- the selection of clear views,
- methods to present histograms,
- coloring schemes.

For the checking of detector performance and of programming tools one needs independent methods. One of the best methods to fulfil this task is visual analysis, which normally can be applied only to a small subsample of the large amount of events recorded in a typical experiment. Visual analysis may even go beyond the capabilities of other methods in recognizing specific event features. It will be shown here, that there are ways of visual data presentation beyond the conventional 2D and 3D techniques, which facilitate these tasks considerably. We will discuss in detail:

- the selection of special representations,
- methods of picture transformation in two and three dimensions,
- the association of tracking information to data of scalar fields (e.g. Lego plot),
- representation of scalar fields in two and three dimensions.

Most of the techniques discussed here were developed and applied for the ALEPH experiment at LEP/CERN [2]. Their direct application to other experimental setups is restricted to cylindrical detectors with a homogeneous solenoidal field. However, it seems possible to modify these techniques for application to different setups. In some cases this will be done here through a generalization of the methods and subsequent application to other experimental devices, namely to tracking detectors outside a magnetic field or experiments without magnetic field.

All techniques mentioned here are incorporated in the graphics program DALI which runs on simple workstations.

2 Pictures for Talks and Papers

Pictures of events are often used in talks and papers to underline and clarify what is said, i.e. to show, what would be lengthy and difficult to explain in words. Such pictures must be easily and intuitively understood, requiring normally only short explanations. The listener or reader should be allowed to assume that his intuitive understanding of the picture is right. It is the speaker's or writer's responsibility to guarantee, that the impression one gets from a picture is the right one.

2.1 Front and Side View

If no event is shown, a detector is best displayed in a technique called cut away perspective view. This resembles a photo of the real detector, where parts of it are cut away to show its interior. For the simultaneous representation of the detector and an event, however, this technique is normally not applicable. In this case the detector is drawn usually in what is called the wire frame technique. Figures 1a and d show perspective projections in this technique.

These pictures, however, are too crowded with lines and need to be simplified. This is done in the *Y* versus *X* projection (*Y/X*: *Y*=ordinate, *X*=abscissa) in figure 1b and in *Y/Z* in 1e. The *Z*-axis is equal to the cylinder axis. Compared to the perspective projections, the number of visible lines in *Y/X* and *Y/Z* is typically reduced by a factor three.

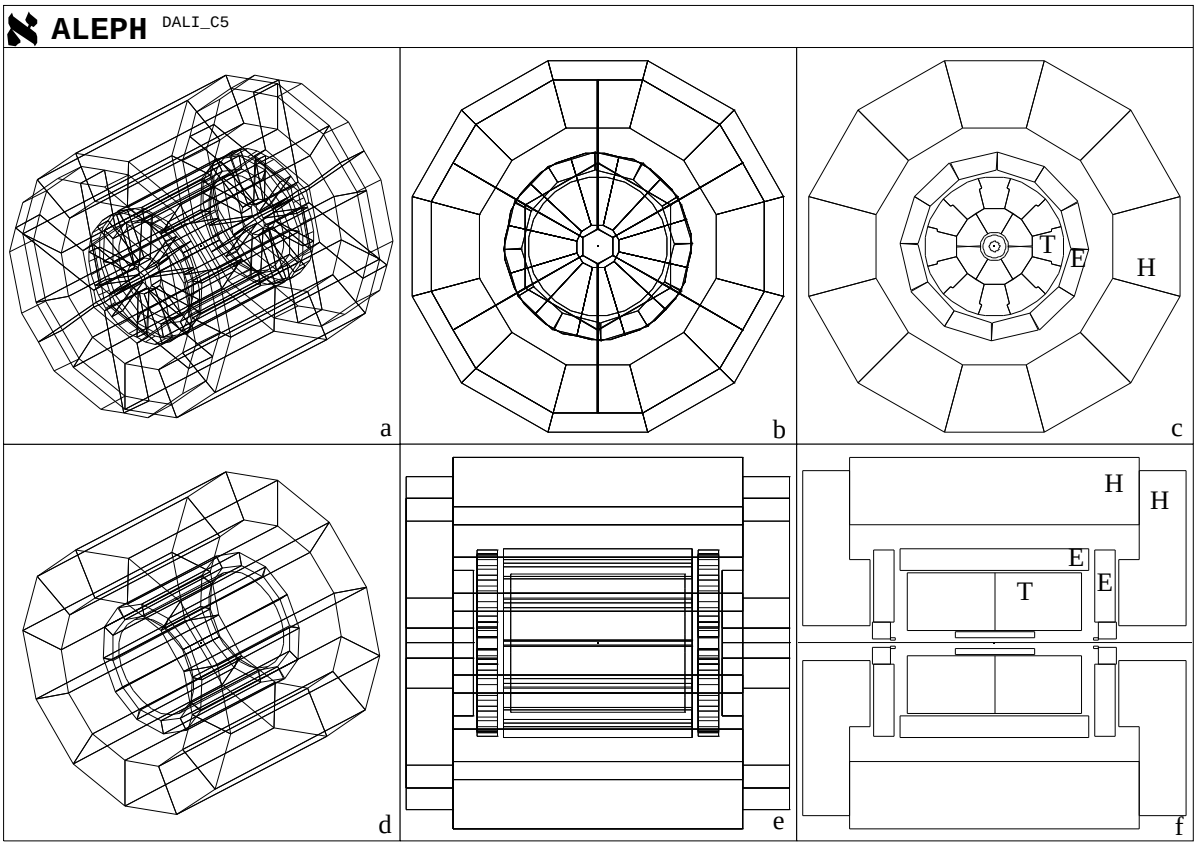

Figure 1: Drawing of the barrel and endcaps of the HCAL(H), ECAL(E) and TPC(T) in the projections:
a) perspective b) *Y/X* c) *Y/X* without endcaps, with TPC sectors
d) perspective without endcaps e) *Y/Z* f) ρ'/Z with inner detectors

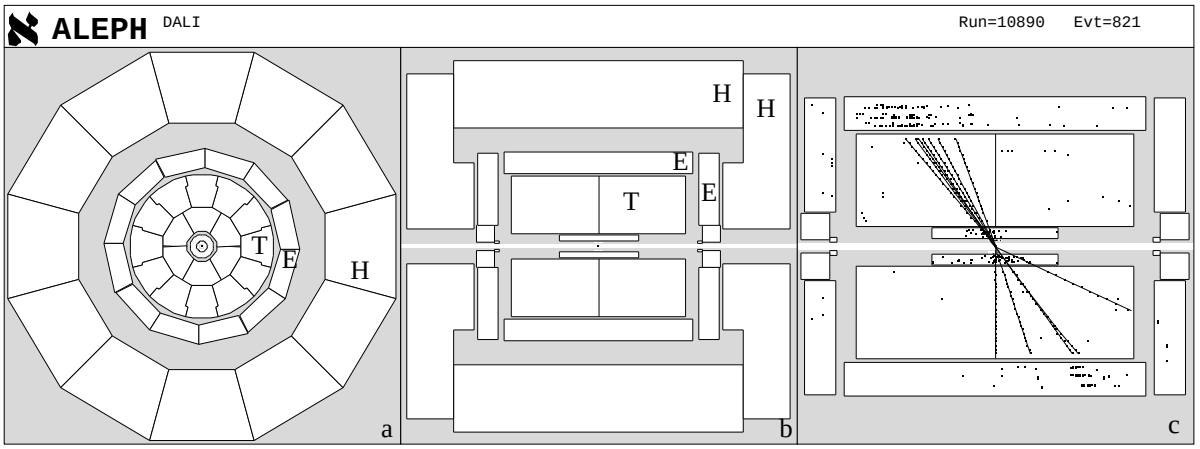

Figure 2: Setting the background to grey
a) *Y/X* b) ρ'/Z c) ρ'/Z of ECAL and TPC with hits and tracks

These projections, however, suffer still from the fact, that different subdetectors are superimposed onto each other[4]. This problem can be solved, if the projections *Y/X* and *Y/Z* are replaced by pictures of cross-sections through the detector center perpendicular (figure 1c) or parallel (figure 1f) to the *Z*-axis.

[4] In *Y/X* the ECAL and HCAL endcaps and the TPC overlap, in *Y/Z* the ECAL,HCAL barrel and the TPC.

However, in such cross-sections events cannot be displayed in a useful way, since a cross-section through a line yields normally only one point. Therefore, one needs projections, which on one side preserve the line character of tracks and on the other side result in the same detector images as the ones obtained from cross-sections.

In the case of the ALEPH detector and of similar ones with cylindrical structure, the *Y/X* projection with endcaps omitted is identical to the cross-section perpendicular to the cylinder axis (front view). This type of picture will be called *Y/X* from now on.

The cross-section parallel to the cylinder axis (schematic side view) is identical to a ρ'/Z projection, where ρ' is defined as $\rho' = \pm\rho = \pm\sqrt{X^2 + Y^2}$ with the sign depending on the azimuthal angle $\left(\varphi = \text{atan}\frac{Y}{X}\right)$ of the object to be drawn; $\rho' = +\rho$, if $\varphi_1 < \varphi < \varphi_1 + 180°$ and $\rho' = -\rho$, otherwise, where φ_1 is interactively defined. In ρ'/Z the event is cut into two unconnected halves (see figure 2c) and even single tracks may be cut into two pieces.

In the case of *Y/X* as defined above, hits in the omitted endcaps are not drawn[5]. For both projections, *Y/X* and ρ'/Z, the following rules hold for the observer:

- hits lie inside the subdetector, from which they originate, so that their source is obvious. That means also, that
- hits or tracks are visible only if the corresponding subdetector is drawn.

  These features, which facilitate interpretation considerably, are lacking in the other projections of figure 1.

The detector elements show up more clearly, if the background around and between them is shaded or colored (compare figures 2a,b to the figures 1c,f and see color plate 1). The presentation of subdetector areas in different colors is improved considerably by overlaying the wireframe, which facilitates the understanding of the structure of the subdetectors. The use of colors or gray shades gives a clear improvement as compared to the mere wireframe picture, especially if a detector section is shown (see color plate 1).

2.2 "Fish Eye Transformations"

In the case of radial symmetric pictures, as the *Y/X* projection of a cylindrical or quasi cylindrical detector such as ALEPH, the scale may be decreased with increasing radius, so that the outer detectors appear shrunk. For a constant total picture size the inner subdetectors are hence enlarged (compare figure 3a and c). This emphasizes the commonly used construction principle of detectors, namely that precision and sampling distance decrease, when stepping from the inner to the outer detectors (see color plate 3).

Such a transformation, which we call "circular fish eye transformation", is calculated in the following way: From the cartesian coordinates *X* and *Y* the spherical coordinates ρ and φ are derived. These are transformed to ρ_F and φ_F by: $\rho_F = \frac{\rho}{1 + a\rho}$ and $\varphi_F = \varphi$. From ρ_F and φ_F the cartesian coordinates X_F and Y_F are recalculated and drawn with a suitable linear scale to conserve the total picture size. The factor *a* is chosen interactively [3].

[5] For the display of tracks going into an endcap, ρ'/Z is the only good, intuitively understandable projection.

The non linear fish eye transformation gets linear for small ρ ($a\rho \ll 1 \Rightarrow \rho \approx \rho_F$) avoiding a singularity at the origin.

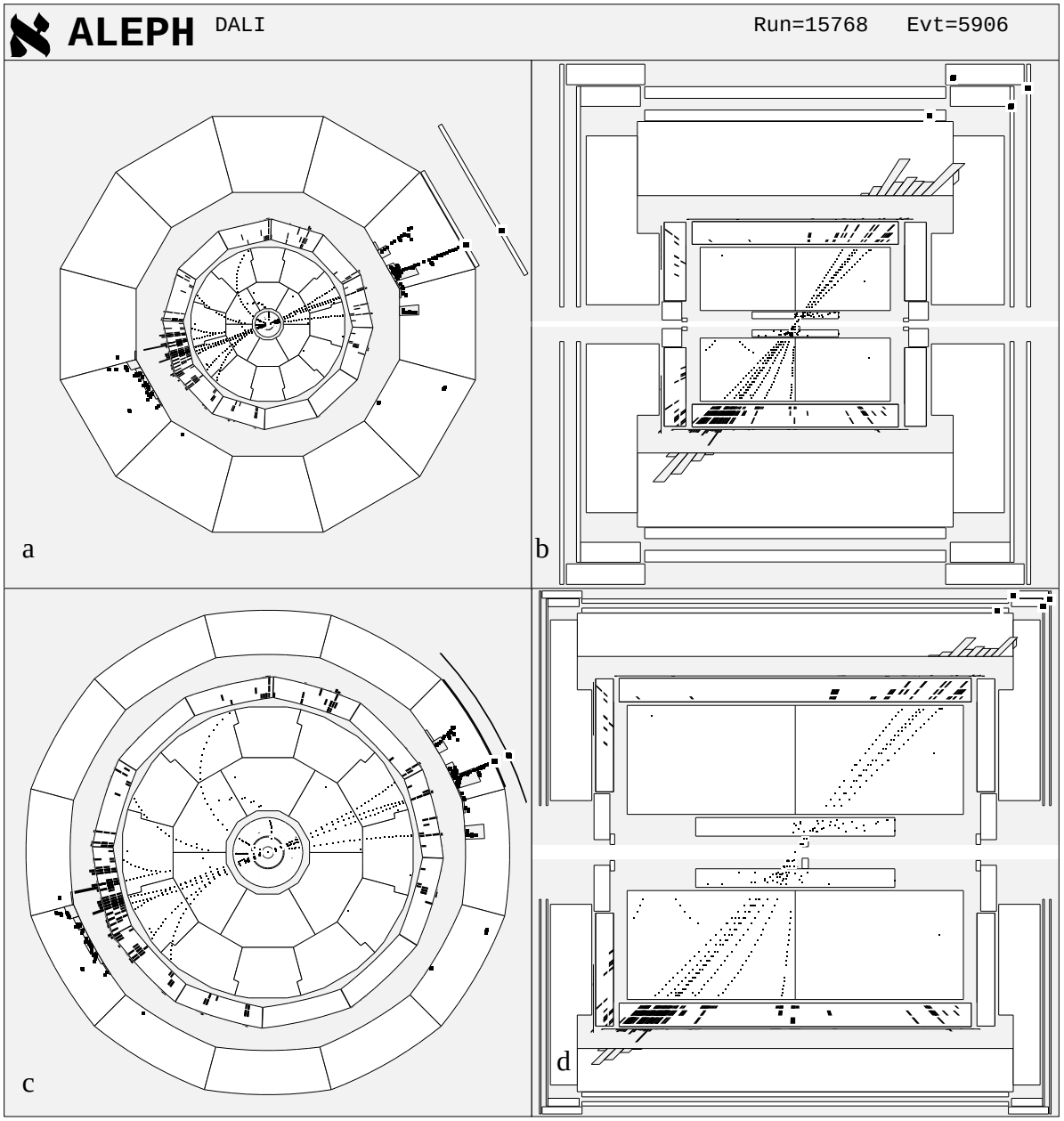

Figure 3: Comparison of linear projections to fish eye projections

a) linear *Y/X*
b) linear ρ'/Z
c) circular fish eye transformation of *Y/Z*
d) rectangular fish eye transformation of ρ'/Z

It transforms circles around the center into circles of another radius. Straight radial lines remain straight with the same angle (compare figure 4 a and b). If this transformation is applied to a picture of rectangular structure, as the ρ'/Z projection in figure 3 b, one gets a picture, which is difficult to interpret, as horizontal and vertical lines get curved (compare figure 4d and 4e).

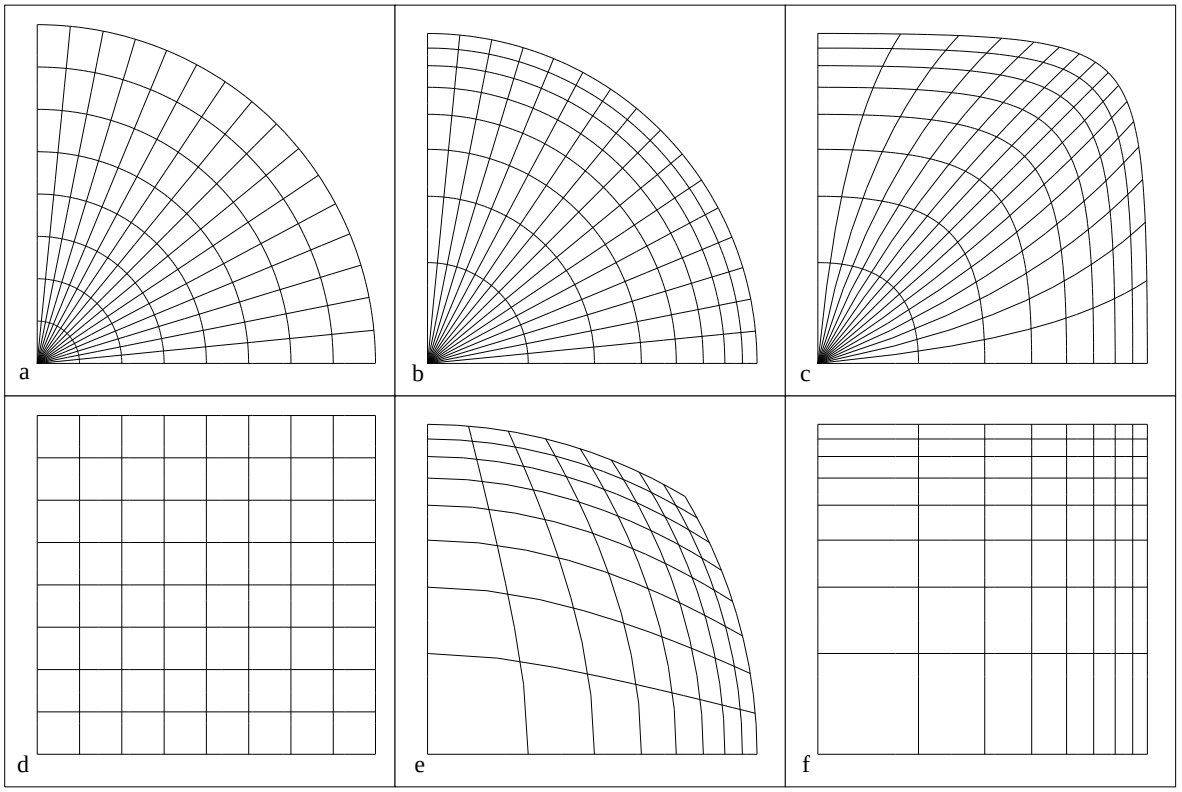

Figure 4: Fish eye transformations of circles and radial lines (a, b, c) and of vertical and horizontal lines (d, e, f)

a) linear b) circular fish eye c) rectangular fish eye
d) linear e) circular fish eye f) rectangular fish eye

The rectangular fish eye transformation of the ρ'/Z projection:

$$\rho'_F = \rho' \cdot \frac{1}{1 + a\rho'} \qquad Z_F = Z \cdot \frac{1}{1 + aZ} \tag{1}$$

transforms horizontal lines into horizontal ones and vertical lines into vertical ones (compare d and f of figure 4). Circles get deformed towards rectangles and radial lines get curved (compare a and c of figure 4).[6] This transformation yields the picture in figure 3d where the tracking detectors are better recognized.

2.3 Histograms in a Picture

Particles showering in calorimeters or just traversing them deposit energy. In order to represent the position of the cells and the deposited energy, the active cells of size Δ_1, Δ_2, Δ_3 and their energy deposit E are commonly displayed by representing them as boxes of size Δ_1, Δ_2, kE, i.e. the length of one side is replaced by the properly scaled energy E.

If a projection is chosen, in which the cells line up behind each other, one gets a picture as seen in color plate 2a which resembles a “wire frame skyline”. This representation differs from a histogram, where the energies of cells lining up behind each other are added. Different modes of presenting such histograms are shown in color plate 2b-2f as wire frame (color

[6] For other detector geometries, analogue transformations can be found

plate 2b), structured wire frame (color plate 2c), unframed area (color plate 2d), framed area (color plate 2e) and structured area (color plate2f). Experience shows, that histograms drawn as structured areas (color plate2f) are preferred by the users. If drawn as wireframe only, the structuring yields a more complicated picture (color plate2c) compared to the unstructured wireframe (color plate 2b).

If histograms are displayed in a picture of radial structure they are best drawn as radial histograms (see Color plates 2 and 3). Even so the detector image is rectangular in ρ'/Z, radial histograms underline better the radial event structure (see color plates 4 and 5).

It may occur, that histograms from different detectors overlay each other. In order not to loose relevant information, four methods may be applied:

- Scaling down of the histograms, in order to avoid overlapping.
- Drawing both histograms as wire frames (see color plate 4a).
- Drawing the first histogram as structured area and the second one on top but as wire frame only.
- Drawing both histograms as structured areas, but in the following sequence: histogram 1, then histogram 2, then the wire frame of both histograms (see color plate 4b, histogram 1 = white, 2 = yellow).

Experience shows, that the last method produces the clearest pictures, but necessitates two passes to draw the same data.

2.4 Application of Colors

The choice of colors depends primarily on the size of the objects to be drawn and on the background, which they are drawn onto. The width of hits and tracks, i.e. points and lines, should be kept sufficiently small, in order to resolve them properly. However, in the case of small objects the human eye distinguishes only very few colors. In other words, it is the number of different colors requested for a display, which defines the object size. A good compromise is the use of the following colors: white or black, green, yellow, orange, red, magenta, blue, cyan and grey (see color plate 6a).

This reduced set of colors is in most cases not sufficient to convey quantitative information (e.g. the depth of an object), i.e. it cannot be used as representation of a third dimension. Colors are however very useful to identify objects on different pictures side by side (see in color plates 5 and compare to color plate 3). This method can even be extended to lists, thus combining pictorial and numerical information. Track separation and association in different views via color is improved, if similar (e.g.close) objects have different colors (see color plates 3 and 5).

2.5 Definition of colors

Objects must be displayed in a way, that they are easily detected and their color is easily identified. For this purpose the display colors of objects and background must be carefully selected.

Any color on a display is composed out of three colors, namely green, red and blue. The contribution of each of these three colors is defined by three independent fractions Fg, Fr, Fb, which represent the intensity of green, red and blue relative to their maximum value. Display screens are normally adjusted such that one gets black, grey or white for $Fr = Fg = Fb$.

The basic display colors are defined in the table below:

color	black	blue	red	magenta	green	cyan	yellow	white
abbrev.	K	B	R	M	G	C	Y	W
Fg	0	0	0	0	1	1	1	1
Fr	0	0	1	1	0	0	1	1
Fb	0	1	0	1	0	1	0	1
Color diff.	B	R-B	B	G-R-B	B	R-B	B	

Table I: Basic display colors

If tiny objects of color Fg_o, Fr_o and Fb_o are displayed on a background of color Fg_b, Fr_b and Fb_b and if the three fractions of one of the sets are increased or decreased continuously, one gets to a point where the objects are hardly visible on the background, because both colors are seen with equal brightness. To avoid this, sufficiently high brightness contrast is necessary for easy object identification [7].

If we compare green and magenta as described in the paragraph above, we find that the brightness of green is substantially higher than the brightness of magenta = red + blue. In the same way we find that red is brighter than blue and yellow brighter than cyan. As colors get brighter if one of its fractions, *Fg*, *Fr* or *Fb*, is increased, the above observations allow to order the basic colors by their brightness. In the table above the brightness of the basic display colors increases from left to right[7]. Ordering the display colors through the well known color circle does not allow to judge the brightness of colors.

The above table and the experience that display colors differing by blue only are poorly distinguishable [8] leads to the following table which summarizes how well objects are separated from the background:

	white	**yellow**	**cyan**	**green**	**magenta**	**red**	**blue**	**black**
white	-	bad	fair	fair	optimal	optimal	optimal	optimal
yellow	bad	-	fair	fair	optimal	optimal	optimal	optimal
cyan	fair	fair	-	bad	optimal	optimal	optimal	optimal
green	fair	fair	bad	-	optimal	optimal	optimal	optimal
magenta	optimal	optimal	optimal	optimal	-	bad	good	good
red	optimal	optimal	optimal	optimal	bad	-	good	good
blue	optimal	optimal	optimal	optimal	good	good	-	bad
black	optimal	optimal	optimal	optimal	good	good	bad	-

Table II: Feasibility of separation and identification of basic display colors relative to each other

[7] The same ordering is used in the test pictures of public TV channels

A second problem arises when one wants to distinguish two tiny objects with color C_1 and C_2. The table above can be applied here as well as a general guide line.

Furthermore, the separation of two objects by their color may depend on the background color. An example is given in a simple test, where a straight line is drawn, with a first part using color C_1 a second part using C_2 and a third part with C_1 again. For comparison a second line with C_2 should be drawn not too close to the first line. If C_1 is set to white and C_2 to yellow, the yellow appears more white on a blue or magenta background and, therefore, the middle part of the first line in yellow is hardly to identify on such a background. The same is true when setting C_1 and C_2 to cyan and green. This effect exemplifies that choosing an optimal background is not trivial.

Special problems, when setting up colors, turn up for printers. Except for its basic colors, which are often identical to the basic display colors, all other colors are produced through dithering, i.e. one recognizes a texture on low end printers. If tiny objects are drawn, picture quality is degraded if the visible size of the texture of objects and of background is not substantially smaller than the size of the objects. Only those parts of the background, where no objects are expected, may be drawn using non basic colors.

2.6 Use of Frames

The color plates 6a,b,c show points of varying size on black, blue and white background. For the representation of small points, a rather dark background is preferable. However, a light background is often preferred for a variety of reasons. Experience shows, that visibility of points is enhanced substantially, if points are surrounded by a thin frame (see color plates 6 d,e,f). The color of small points surrounded by a white frame and drawn onto dark background is often difficult to recognize, as the points seem to be white. For large objects however, a white frame improves recognition considerably, e.g. for blue objects on black background.

Due to the frame, the effective size of points or lines increases, which leads to a loss of resolution. This is overcome by drawing first all frames and in a second pass all points and lines. This is demonstrated in color plate 7 with a blow-up of 4 tiny points drawn on black and white background without frame (a), drawn sequentially, i.e. frame, point, frame, point... (b), and drawn in two passes (c). Experience shows, that resolution is not decreased in this way, but framing deteriorates recognition in regions with a high density of data, e.g. the inner (black) detector in color plate 3.

The methods described until now lead to a picture as seen in color plates 3 and 5, which are fairly easy and fast to understand.

3 Visual Analysis

In most experiments a large number of events are stored. It is often necessary to examine visually a subset of these events for a variety of reasons, as e.g.:

- check of hardware and software (on- and off-line)
- check of selected events,
- intuitive understanding of events and of possible problems,
- search for suitable events for talks and papers.

The examination should be effective and unbiased. However, one cannot assume that the intuitive impression one gets from the picture is right, in contrast to the situation, where one is looking at a picture presented in a talk or paper. One may be mislead for several reasons:

- loss of information,
- false assumptions,
- suggestive results.

In short: what looks good, may be wrong.

In the following we will discuss a variety of different representations, which help to avoid misinterpretations. Starting with representations of two dimensional data we will concentrate then on how to represent three dimensional data.

3.1 Use of picture transformations

It is common use in physics, particularly when handling multi-dimensional data, to apply suitable non-cartesian projections in order to better visualize the data, e.g. transverse versus longitudinal momentum, P_T/P_Z, which corresponds to ρ/Z in coordinate space. The choice of these projections depends strongly on the data to be displayed. A well known example is the application of logarithmic scales. It may be regarded as a non linear picture transformation and is particularly powerful for the examination of exponential curves, which are linearized (compare figures 5a and d) taking advantage of the fact that human perception can better judge and extrapolate straight lines than curved ones. In contrast to the original picture in figure 5a, the change of exponent is clearly visible in the logarithmic representation of figure 5d.

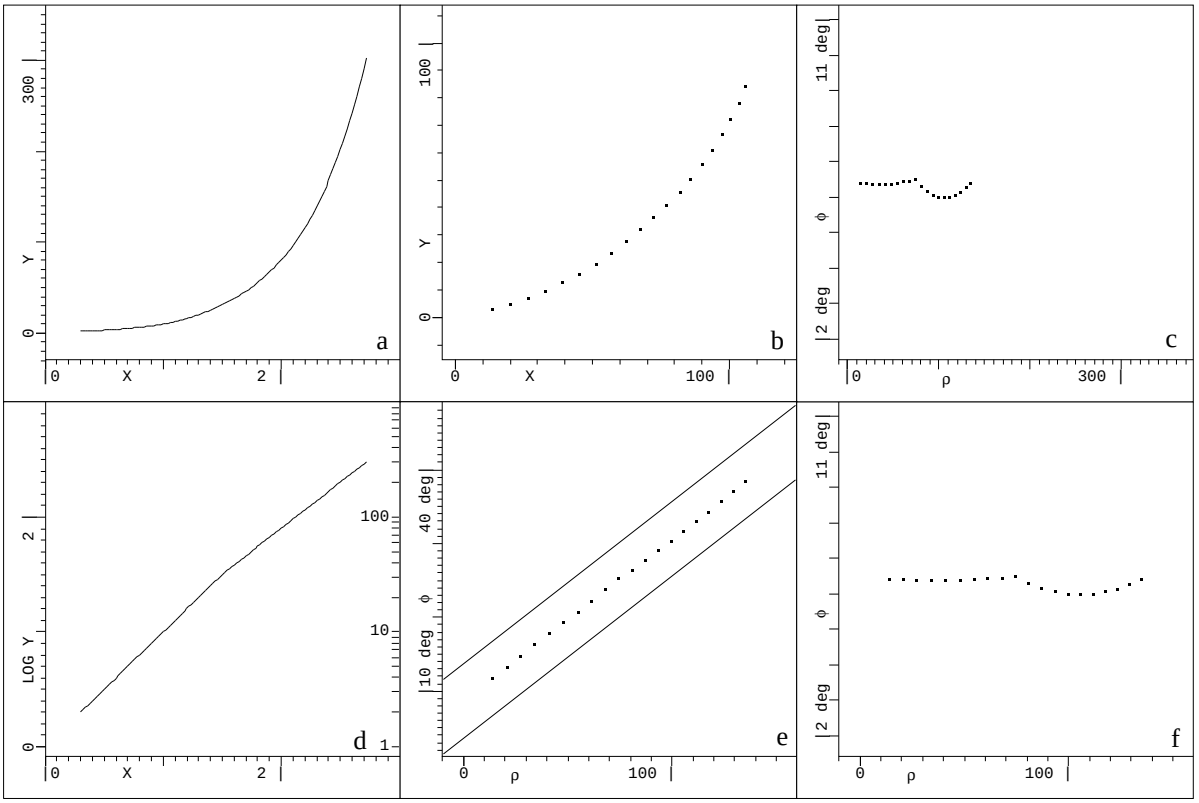

Figure 5: Linearization of an exponential curve and of a segment of a circle

a) exponential curve b) segment of a circle c) compressed φ/ρ
d) same curve as (a) in log. scale e) same segment as (b) in φ/ρ f) linear transform. of φ/ρ

It will be shown below that segments of circles (figure 5b) can be linearized by a φ/ρ projection (figure 5e). Through subsequent linear transformations it is possible to enhance features, which are otherwise difficult to extract (see the kink in figure 5f and c). These and similar methods will be discussed in the following.

3.2 Helices in Cartesian and Angular Projections

Due to the radial event structure and the cylindrical detector structure it is of interest to investigate the use of angular projections, i.e. of projections based on cylindrical and spherical coordinates[8]. The ρ'/Z projection discussed above may also be regarded as an angular projection.

In many detectors, such as the LEP detectors, tracks of particles are recorded, which move in a homogeneous solenoidal magnetic field parallel to the *Z*-axis. These tracks are described by helices. In order to better understand the use of angular projections, the helix equations will be formulated in cylindrical and spherical coordinates.

Neglecting multiple scattering, charged particles of momentum $\vec{\vec{P}} = \left[P_X\ P_Y\ P_Z\right]$ passing through a solenoidal field move along helices. Assuming that they start from the collision point at the origin of the coordinate system, the helices may be described in cartesian and in spherical coordinates as function of $\Delta\alpha = 2\Delta\varphi$ in the following way:

$$\begin{aligned} X &= cP_T\,[\cos(\alpha_0+\Delta\alpha) - \cos\alpha_0] \\ Y &= cP_T\,[\sin(\alpha_0+\Delta\alpha) - \sin\alpha_0] \qquad \text{with } \alpha_0 = \varphi_0 + 90^\circ \\ Z &= cP_Z\Delta\alpha \qquad\qquad\qquad\qquad\qquad\qquad Z = 2cP_Z\Delta\varphi \end{aligned} \tag{2}$$

$$\begin{aligned} \tan\varphi &= \frac{Y}{X} \qquad \rho = \sqrt{X^2+Y^2} \qquad R = \sqrt{X^2+Y^2+Z^2} \qquad \tan\vartheta = \frac{\rho}{Z} \\ \tan\varphi_0 &= \frac{P_Y}{P_X} \qquad P_T = \sqrt{P_X{}^2+P_Y{}^2} \qquad P = \sqrt{P_X{}^2+P_Y{}^2+P_Z{}^2} \qquad \tan\vartheta_0 = \frac{P_T}{P_Z} \\ \varphi &= \varphi_0 + \Delta\varphi \qquad \rho \approx 2cP_T\Delta\varphi \qquad R \approx 2cP\Delta\varphi \qquad \vartheta \approx \vartheta_0 \end{aligned} \tag{3}$$

the above approximations are valid for $\sin\Delta\varphi \approx \Delta\varphi$. Most particles have a sufficiently large momentum to justify this approximation, i.e. their track radius is sufficiently large.

Figure 6a shows 6 tracks in *Y/X*, where helices give circles, the radius of which is proportional to P_T. The *Y/Z* projection of the same tracks leads to cycloids as seen in figure 6b. It can be seen from the equations (3), that as long as $\sin\Delta\varphi \approx \Delta\varphi$, helices are linear in the angular projections φ/Z, φ/ρ and φ/R (figure 6d, e and f). Their inverse gradient is proportional to P_Z, P_T and *P* respectively. In ρ'/Z (figure 6c) they are straight. In projections where any variable is drawn versus ϑ, e.g. φ/ϑ (6g), one gets approximately straight, vertical lines. The approximation fails for helices which do not pass through the center and for helices with many turns. As long as a helix with many turns passes again through the *Z*-axis, it is

[8] The most famous of such projections is the Mercator projection, which deals with the spherical structure of the earth.

described in φ/Z by a set of parallel straight lines (see track 2 in figure 6d). Particle momentum and charge cannot be estimated from the projections *Y/Z*, ρ'/Z and φ/ϑ.

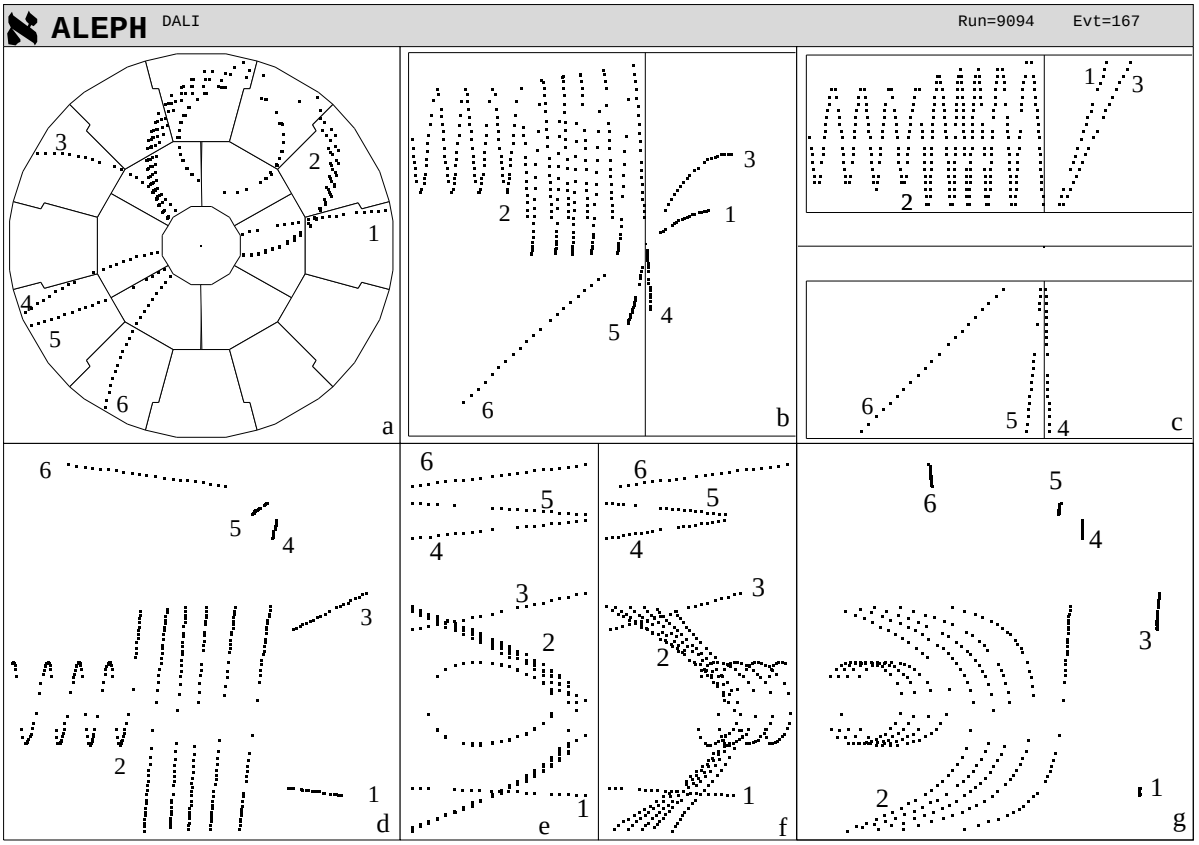

Figure 6: Helices in cartesian and angular projections

a) *Y/X* b) *Y/Z* c) ρ'/Z

d) φ/Z e) φ/ρ f) φ/R g) φ/ϑ

The φ/ρ projection is particularly useful to extrapolate tracks into the barrel part of calorimeters, whereas φ/Z is the best projection for extrapolation into the endcap part. This is due to the fact, that in projections of any variable versus ρ the barrel parts of different detectors are separated on the picture, whereas in anything versus Z the endcaps are separated, so that the rules of chapter 2.1 can be applied. φ/Z is preferable to *Y/Z*, as the longitudinal momentum P_Z and the charge of the particles can be estimated.

3.3 Lines through Sequences of Points

In the pattern recognition programs the hits belonging to a track are searched for and a helix is fitted to them[9]. In color plate 8a three helices are drawn suggesting the existence of three independent tracks. The helices were derived from a fit to the hits seen in color plate 8b. However, the picture shows that two of the tracks belong together, as incoming and outcoming track from a decay of a charged particle, yielding a so called “kink”. Color plate 8c shows in another example a set of hits, which were joined by the pattern recognition program to two

[9] In reality the fit may take into account multiple scattering leading to a curve which is only approximately a helix.

tracks, shown as lines. Although this assignment looks very convincing, it turns out to be less obvious, if only the hits are drawn (color plate 8d). A better way to show the hits together with their track assignment while avoiding the suggestive force of lines is to color the points according to their track assignment (color plate 8e).

The examples above demonstrate, that it is necessary to recognize tracks from their hits only. Therefore we need to understand how human perception connects a sequence of points to lines.

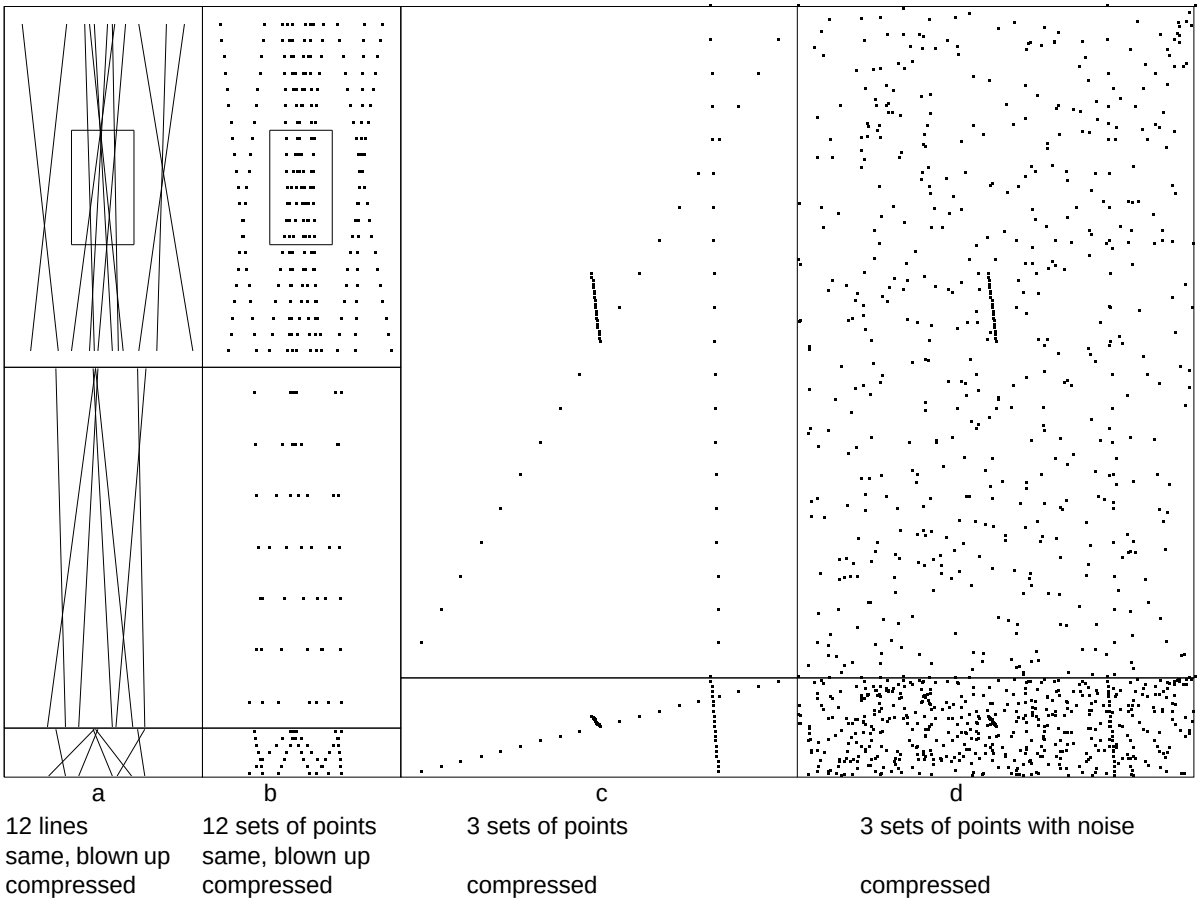

Figure 7: Track recognition by the human brain

To this purpose figure 7a displays 12 straight lines and in figure 7b the same lines formed of a sequence of points. In the blow-up of the crowded center region of figure 7a seven lines are easily distinguished. However, if the lines are drawn as a sequence of points and blown up (7b), the seven vertical lines are hardly identified. If, however, the picture is compressed in the direction of the lines (see bottom of figures 7b), the lines are easily identified, even if only drawn as points.

Figures 7c and d show the same 3 straight lines of rather different direction and length in a clean (7c) and a noisy (7d) environment, where in the latter case the two long lines with large spacing between neighbouring points are lost. Compressed pictures are shown at the bottom of these figures. In the noisy environment, the line in the direction of the picture compression is easily identified, contrary to the two other tracks, of which the long one was not compressed and the short one was “over compressed”.

One learns, that human perception identifies a line from a sequence of points by joining close points together and not by following - like a computer - a predefined mathematical function.

In the case of events of radial structure, there is no preferred direction of compression if one wants to visualize the total event (see figure 8a). However, there are methods of radial compression, e.g. the fish eye view (see figure 8b). The principle of such methods can be summarized as follows: the angle under which a point is seen from the center remains unchanged, but its distance from the center ρ is changed via a suitably chosen function to $\rho_{NEW} = F(\rho)$, e.g. $\rho_{NEW} = a + b\rho$ with $a > 0$ and $0 < b < 1$.

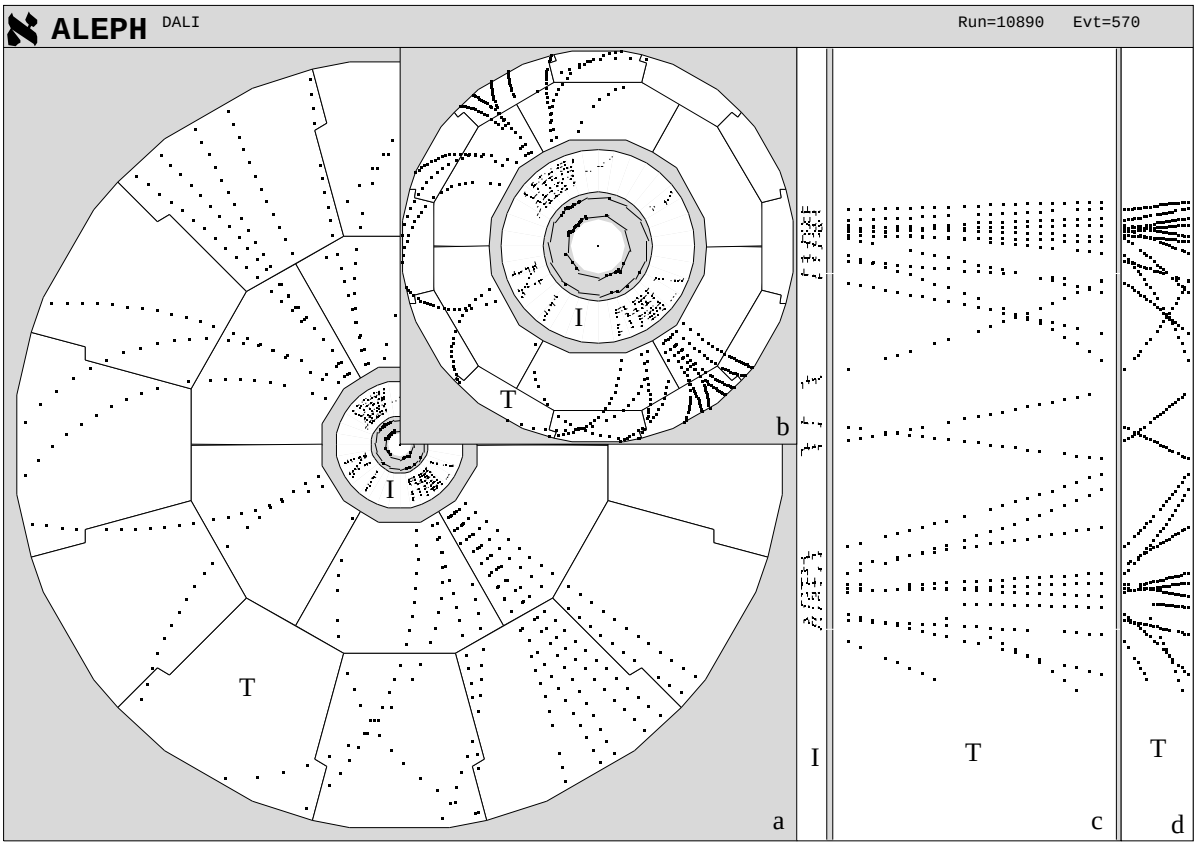

Figure 8: 2π compression of a total event in the ITC(I) and the TPC(T)
a) *Y/X* b) fish eye compression c) φ/ρ d)compressed φ/ρ

A more powerful method consists in "unrolling" the picture to the φ/ρ projection (see figure 8c) and compressing it (see figure 8d) in ρ direction.

3.4 Blow-up of a sequence of points

In many detectors hits are recorded with very high precision. In the ALEPH TPC hits are recorded with a sampling distance of $d = 60\ mm$ and a precision of $\Delta = 180\mu$. In order to visualize errors of this size on a screen, one must blow up the interesting part of a picture such that 1 pixel corresponds to 180μ at least. As a consequence a screen image with typically 1000 x 1000 pixels covers only a detector area of $180 \times 180 mm^2$ in the case of a symmetric magnification (*aspect ratio = 1*). Therefore one ends up with only very few points on the

screen, i.e. one looses the relevant context to all the other hits of the track. This gets even worse for detectors of higher precision.

If one is only interested in the errors perpendicular to the track direction, a small magnification in track direction and a high one perpendicular to it (*aspect ratio > 1*) yield a picture, on which many hits are visible as well as their deviation from a smooth track. Color plate 9a displays a section of *Y/X* with *aspect ratio = 1*. The rectangle shows a section, which is blown up to give the picture in color plate 9b with an aspect ratio defined by the sides of the rectangle.

However, if tracks are rather curved, they can only be contained in a correspondingly large rectangle, which means, that the magnification perpendicular to the track is limited. This can be overcome by first linearizing the track using φ/ρ (color plate 9d) followed by a sufficiently large linear transformation. As an example, the parallelogram[10] containing the tracks as seen in color plate 9d is transformed to the full size of the square picture (color plate 9e), where the scattering of the hits is now clearly visible.

A magnification can be reached (color plate 9e and f), which yields a picture similar to a residual plot (color plate9c, upper part). The residual plot, however, has the disadvantage not to show hits of other tracks or isolated hits close by. Note the use of colors to associate the hits between color plates 9c and f.

In essence it turns out that through such methods the limits due to the resolution of the screen and of the human visual system can be overcome.

3.5 Visualisation of the Vertex Region and the Inner Detectors

It is sometimes required to blow up track images near to the vertex region, e.g. for the investigation of secondary vertices close to the vertex. This can be accomplished by a linear blow-up or by use of the fish eye transformation (see chapter 2.2), which allows to visualize the tracks further away from the centre as well. Close to the vertex, i.e.in the region of interest, it yields a picture similar to a linear blow-up, so that distances and correlations can be estimated correctly.

3.6 Imaging Events from Fixed Target Detectors

In many detectors, particularly in fixed target detectors, particles leave the interaction point in a preferred direction. Two questions, arising when visualizing such events, will be discussed here:

- How to estimate visually, by which amount straight tracks point beside the interaction point? This problem arises in experimental setups, where tracks are curved by a magnetic field but recorded in a detector further down outside the magnetic field.
- How to show simultaneously tracks in small subdetectors close to the center and large subdetectors further downstream?

The top of figure 9a shows a simulation of hits recorded outside a magnetic field. The amount by which the tracks point beside the interaction point is a function mainly of the particle momentum, which is of main interest. However, due to the large distance of the hits from the interaction point it is rather difficult to estimate this quantity from the picture without relying

[10]Using the rubber band technique, the parallelogram and the rectangle are defined interactively in any direction.

on a pattern recognition program providing straight lines for backward extrapolation as in the bottom of figure 9a.

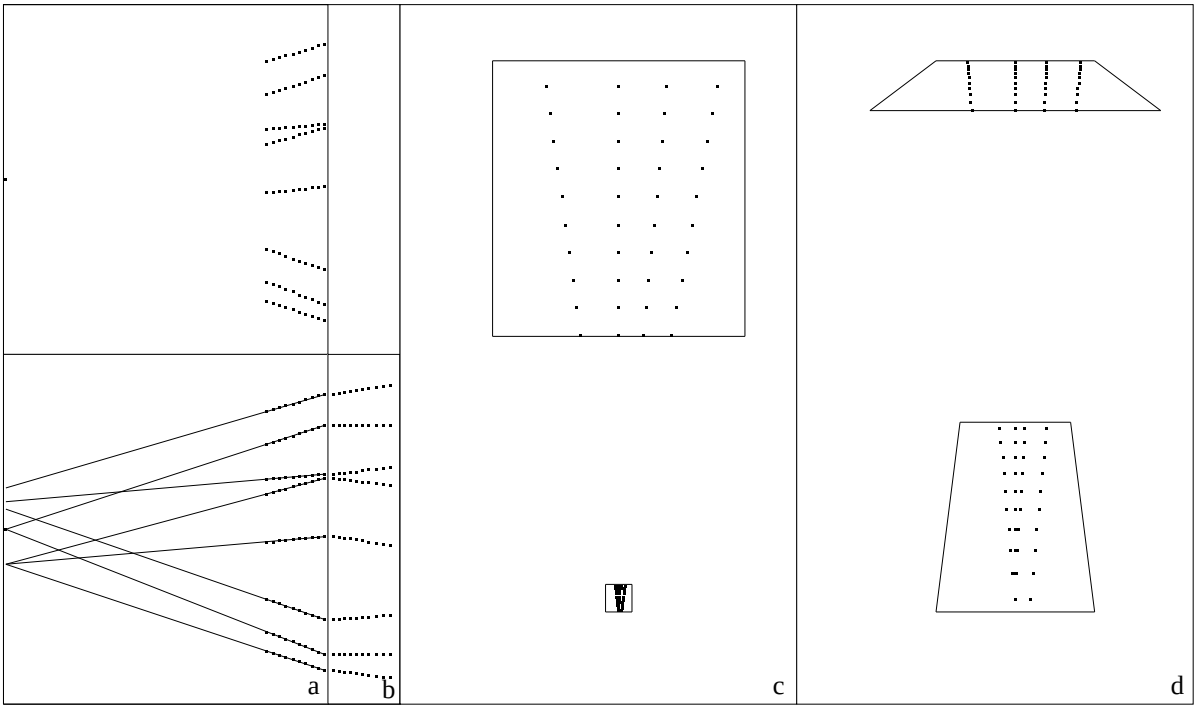

Figure 9: Non linear transformations of straight track segments
a) *Y/X* b) Y'/X' c) *X/Y* d) X''/Y''

The tracks can be described by $Y = a + bX$, where X is the downstream axis. As mentioned above, the offset, a, depends mainly on the particle momentum and only very slightly on the track direction, unlike the gradient, b, which depends on both. The equation can be rewritten as $Y' = \frac{Y}{X} = \frac{a}{X} + b = aX' + b$. One sees that the non linear transformation $X' = \frac{1}{X}$, $Y' = \frac{Y}{X}$ transforms straight lines into straight lines. They are shown in Y'/X' in figure 9b[11]. From the gradient *a* of these lines the particle momenta can thus be locally estimated even in cases where the center point and the hits cannot be displayed simultaneously.

By further application of linear transformations one can derive a more general formulation $X'' = \frac{X}{1 + cX}$, $Y'' = \frac{Y}{1 + cX}$, which again leaves straight tracks straight [3]. This transformation corresponds to the picture formed in our eye, when looking with a grazing view onto a flat image[12]. Figure 9c shows a picture - X/Y - from two subdetectors of very different size with 4 straight tracks. In X''/Y'' (9d) the tracks remain straight, but can be resolved in both subdetectors, and the track segments can be connected by a straight line. This transformation can also be applied to curved tracks. If only slightly curved, the track images are practically identical to those obtained from the fish eye transformation discussed before.

[11]The Y'/X' projection was properly scaled.
[12]If $Y \ll X$, X can be replaced by ρ leading to the fish eye transformation discussed before.

3.7 Island Representation of Calorimeters

Calorimeters are composed of cells, in which energy is deposited either by the traversing particles or by their showers. These cells may be grouped together in layers surrounding the inner part of the detector (see the three layers of points in the outer ring shown in figure 10a). The optimal projection for the representation of these layers depends on the geometrical structure of the calorimeter. The electromagnetic and hadronic calorimeters in ALEPH have a projective structure, i.e. neighbouring cells of different layers can be grouped into towers, the axis of which points to the center of the detector, as well for the barrel as for the endcap. This suggests the use of φ/ϑ to display single layers, as:

- barrel and endcap can be shown on the same picture,
- pictures of different layers have the same geometrical structure.

In figure 10a hits lying in a given solid angle are shown. The same hits are shown in φ/ϑ for layer 2 and 3 in figures 10b and c, respectively. The amount of deposited energy per cell is proportional to the size of the squares inside the cell. In order to analyze the shower development between these two layers, the active cells - cells with deposited energy - in layer 2 must be compared to the corresponding ones in layer 3. This is facilitated considerably, if only towers are drawn, which have active cells in at least one of the three layers (see figures 10d,e,f) [4]. This yields an irregular, island like substructure identical in all three images, which helps to correlate intuitively the cells in the different layers to each other.

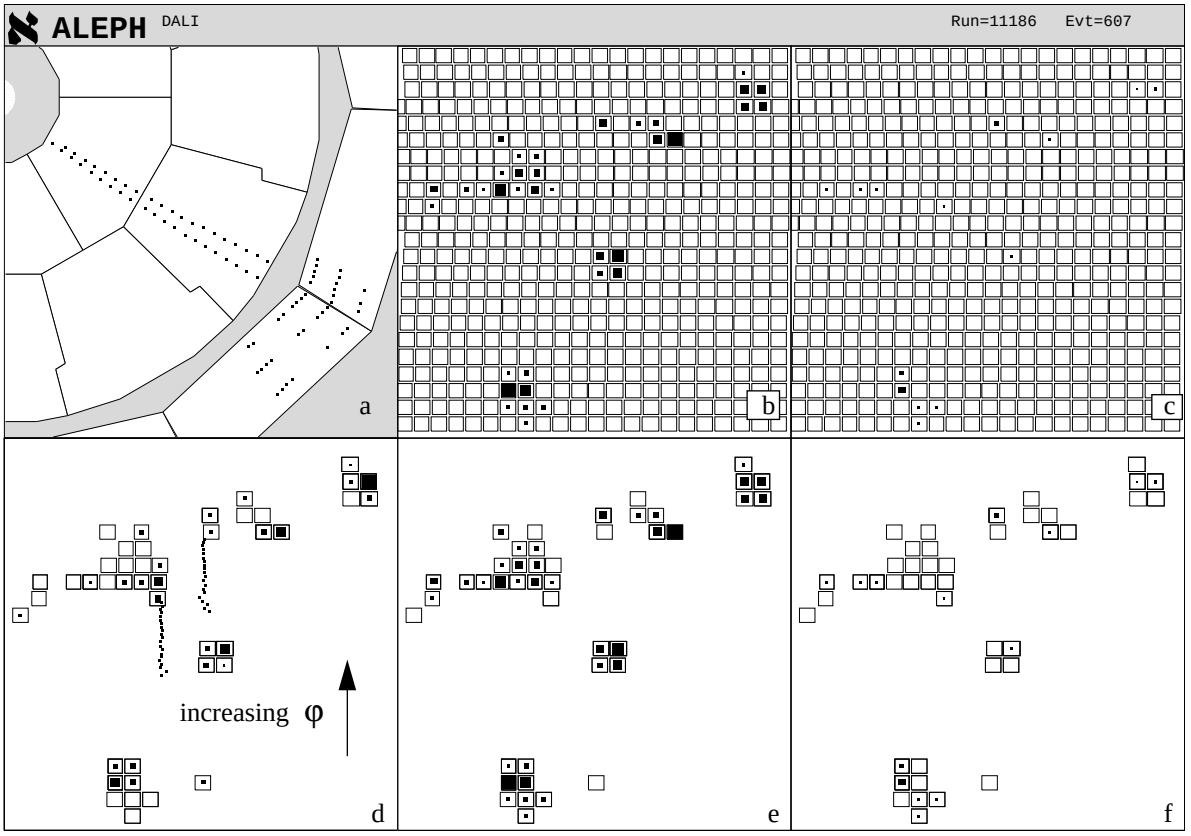

Figure 10: Display of tracks and calorimeter data in *Y/X* (a) and φ/ϑ (b-f) (The area of the solid squares is proportional to the deposited energy).

a) Y/X
b) Full structure of layer 2
c) Full structure of layer 3
d) Island structure of layer 1 and TPC tracks
e) Island structure of layer 2
f) Island structure of layer 3

The next problem is how to associate tracking information to the calorimeter information, i.e.tracks to showers. In *Y/X* shown in figure 10a, the track to shower correlation is not obvious, due to the missing *Z*-information and to the overlap of showers lying behind each other. If φ/ϑ is used instead, two methods may be applied:

- A track fit is made to the tracks, and the entry point into the first layer is displayed. In this case one relies on a good track recognition and fit. The direction under which particles enter the calorimeter is not visualized.
- The hits of the TPC are superimposed in a φ/ϑ projection onto the first layer (see figure 10d). This method is rarely used, as further information is needed for an unambiguous analysis. In this representation there is no information, whether the azimuthal angle φ increases or decreases for the tracks, e.g. whether the right track seen in figure 10d is associated to the island above or below. For this and other reasons it is necessary to use additional projections and reliable methods of track correlation between the different projections.

Particle momentum and charge cannot be estimated from φ/ϑ. This problem and the difficulties when applying the second method, are caused by the fact that only two dimensional projections are applied. In the next chapters possible solutions to represent the full three dimensional information will be discussed.

4 Three Dimensional Representations for Visual Analysis

Many (sub-) detectors record the position of hits in three dimensions. Here we will assume, that the errors of all three measured coordinates are sufficiently small, so that patterns of tracks or showers can be meaningfully visualized in any projection.

For the representation of such data we will try to find single pictures or picture sets, which allow to extract all relevant information. Several methods are used to solve this problem:

- perspective projections, sometimes called 3D,
- volume rendering, shading etc.,
- smooth rotations on appropriate 3D-stations,
- stereo pictures on appropriate stereo stations,
- technical drawings showing front, side and top views,
- abstract methods applicable for special sets of data.

The application of these methods for visual event analysis will be discussed in the following.

4.1 Perspective Projections.

Figure 11a shows a two dimensional wire frame projection of two objects, which we interpret as being three dimensional cubes. In doing so, we apply more or less strictly a set of assumptions, namely

- Straight lines on the picture are straight in space.
- Each line represents one line only, i.e. it is not composed out of several lines, overlaid or just touching on the projection.
- Lines parallel on the picture are parallel in space.
- Lines touching each other at a corner, touch each other in space.
- The angles between lines at the corner are angles of 90°.
- Several discrete line segments lining up on the picture do so in space.

As a consequence we see two cubes in figure 11a. But there exists an infinite number of three dimensional objects, which yield the same two dimensional image. One such object, for which the above assumptions are not fulfilled, is seen in figure 11b, from which the "cube" in figure 11a is obtained by a rotation of 20° around a vertical axis in the picture plane. If we see a picture like the one in figure 11a, we prefer automatically the most familiar solution. However, we can only be sure that this interpretation is right, if we know beforehand, that the above assumptions are valid, i.e. that we know beforehand, that we see two cubes.

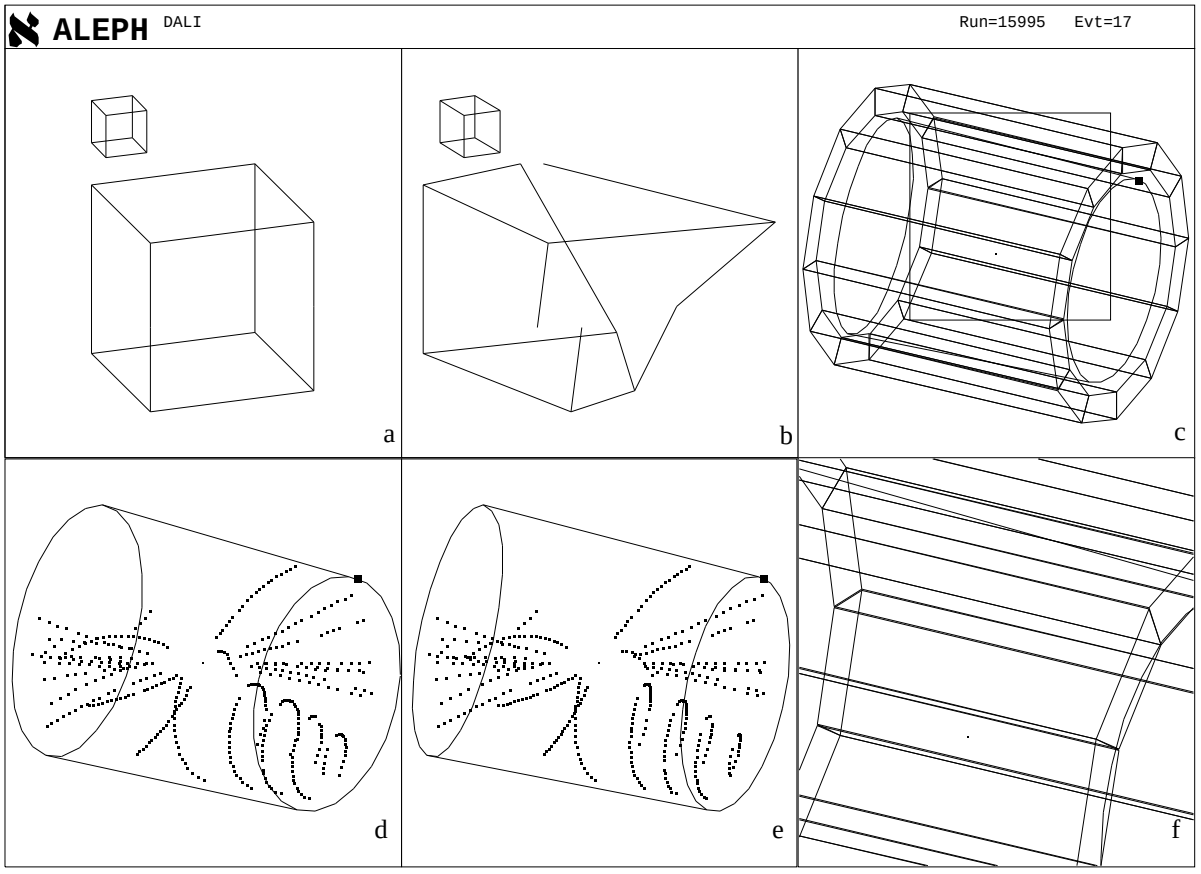

Figure 11: Perspective projections of
a) two "cubes" b) two "cubes" rotated by 20° c) TPC + ECAL
d) TPC + event (left eye) e) TPC + event (right eye) f) TPC + ECAL blown up

If we know, that what we see is a cylinder, we can reconstruct a three dimensional cylinder in our brain from a two dimensional projection of it. Therefore, a two dimensional projection of a detector, of which we know what it looks like, will form a three dimensional image in our brain (see figures 11c,d,e).

However, if we look at points or at lines of the picture of an event, no one of the above assumptions is valid a priori. For an event there is no way to estimate the depth of points and tracks (see figure 11d), i.e. the picture of the event remains two dimensional. Furthermore, one may be mislead by basing a decision on the preference of the simplest solution, which is even reinforced, if a two dimensional projection of hits and tracks is combined with a three dimensional detector image. An exception are points (e.g. confirmed end points of tracks) from which we know, that they lie on a plane. If this plane is surrounding a volume, one gets two solutions, one for the front and one for the back plane.

The advantage of showing the detector lies in the fact, that the direction, from which we are looking, is visualized. Furthermore one transmits the information, that the data are three dimensional.

A problem arises, if a part of the picture is blown up in a way that the lines, which compose the cubes, the cylinders etc., are unconnected. In this case the assumptions above, even if valid, cannot be applied, so that a rather complicated picture results (see figure 11f).

In the case, that the event and not the detector is of main interest, we can conclude that, what is often called 3D, is in reality a 2D projection not able to convey all relevant information. There are classical methods to improve this situation, namely the combination of perspective projections with

- shading and volume rendering,
- smooth rotations,
- stereo pictures.

They will be discussed in the following.

4.2 Shading and Volume Rendering

The picture of an event consists of

- points and lines, representing hits and tracks, which must be kept thin, in order not to loose resolution for the display of many of them, and of
- rather small boxes representing calorimeter cells, where often cells lie behind each other.

In the first case volume rendering techniques cannot be applied as we cannot distinguish enough intensity grades or colors on small objects. In the second case the wire frame technique must be applied if cells should not be obscured. This excludes shading and volume rendering except that very few hits and tracks are drawn.

If shading and volume rendering are applied to several subdetectors surrounding each other, one is lead back to cut away perspective views, onto which a two dimensional projection of an event can be overlaid, but the hits or showers of the event do often not correspond to the subdetectors they are drawn onto. One may find simple events which allow this, but for visual analysis, which must cope with all kind of events, these methods seem not to be applicable.

4.3 Smooth rotations.

One of the best methods to get additional information about three dimensional objects from a two dimensional display is a smooth rotation around an axis the direction of which is

sufficiently different from the viewing direction. During rotation the three dimensions of the data are mapped onto three independent variables, i.e. their horizontal and vertical picture position and the speed of displacement.

When applying a small smooth rotation, it is possible to identify hits, tracks or track segments, which are close to each other, as they move with similar speed. In many cases this is insufficient, as the lateral displacement of the projection of a point is generally much smaller than its depth in space.

If one rotates by 90° one gets a smooth transition between two distinct views, which helps to associate the images of hits and tracks on the first view with their corresponding images on the second one. However, for high multiplicity events, this method of association becomes rather tedious. It will be shown in chapter 4.5, that three orthogonal views are needed in more complicated cases, i.e. rotations around different axes are required. Thus a thorough check of an event becomes time consuming and requires a fair amount of discipline from the operator. A special case is treated in chapter 5.

4.4 Stereo Images

If we one looks at the data presented in one way or the other in real 3D, e.g.on a stereo device, one understands better the detector picture and the event structure and one can confirm the assumptions of chapter 4.1. The display of the detector image helps considerably, as it gives the necessary information of the depth scale. As each of our eyes is a 'two dimensional image recorder', smooth rotations help us further to match the points and lines from the two images in our brain.

However, due to the relatively small eye distance as compared to the distance between our eyes and the objects, depth recognition, when looking at things, is considerably worse than lateral recognition. Therefore, we are unable to judge the curvature of a track, if it is curved in a plane through our eyes. These observations are easily confirmed with real objects.

From the figures 11d and e one gets a stereo image, if one succeeds to look at the left picture with the left eye and the at the right picture with the right eye. By comparing the two images one may estimate the tiny differences, which lead us to recognize a stereo image.

4.5 The Method of Technical Drawings

A commonly used method of representing three dimensional objects is found in technical drawings, where three orthogonal projections are used, normally the top, front and side view. In figures 12a,b,c five specially selected tracks are shown in the top (*Y/Z)*, front (*Y/X)* and side view (*X/Z)*. Apart from a small change in length, the group of three tracks (2,3,4) gives the same image in the top and front view, whereas they look very different in the side view. Contrary to them, the curvatures of tracks 1 and 5 are similar in the front and side view, but look different in the side view.

For a thorough check of a track - or a set of nearly parallel tracks - two projections are required, one where the track is seen curved and one where it looks practically straight. In the case of an event, where tracks go into many directions, at least three projections are required, as in the example above. This means that the event must be rotated around several axes.

However, the front view (Y/X) (see figure 12b) and the schematic side view, i.e. the non linear ρ'/Z projection, (figure 12d) show all tracks from the side with the maximum and minimum apparent curvature, respectively[13]. Therefore, the top, front and side view can be

replaced by the two "orthogonal projections" Y/X and ρ'/Z for tracks pointing roughly to the center.

Very close to the center, the radial event structure is normally broken due to measuring errors or possible secondary vertices, so that the interpretation of ρ'/Z becomes difficult. It should be further kept in mind, that momentum conservation cannot be checked in this projection.

Even the use of two projections instead of three suffers from the fact, that one has to associate hits and tracks in one picture to their image in the other one. Therefore, it will be tried in chapter 6 to show ways of presenting three dimensional data in one picture only, using unconventional but less intuitive projections.

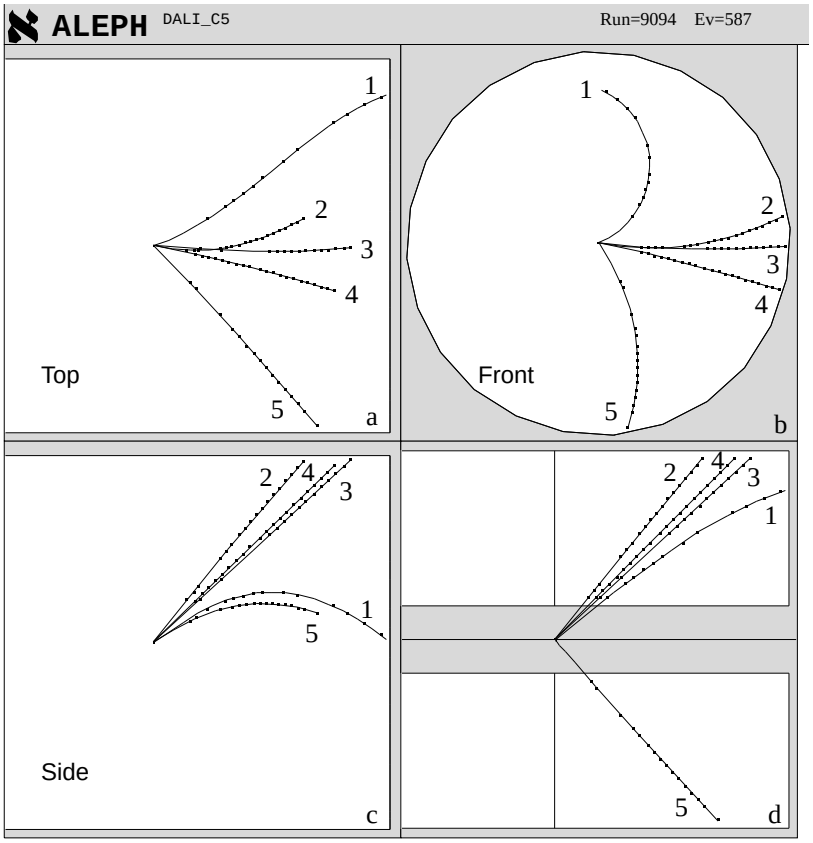

Figure 12: Top, front and side view and ρ'/Z of five selected tracks

a) top view (*Y/Z*)
b) front view (*Y/X*)
c) side view (*X/Z*)
d) schematic side view ρ'/Z

For all methods of 3D data representations discussed so far, it is difficult to find solutions of simultaneous data compression of the total event, as discussed in chapter 3.3 for 2D representations

5 Track Visualisation Close to the Primary Interaction Point

A special problem arises when examining secondary vertices near to the primary interaction point. Secondary interactions may manifest themselves by tracks crossing or nearly crossing at

[13] This is due to the fact that a track looks straight in Y'/Z with $Y' = Y\sin\alpha + X\cos\alpha$, if α is chosen such that the track lies approximately in the picture plane, which means $Y' \approx \rho'$.

a point different from the primary interaction point. The distance between these two points is of main interest for physical analysis.

The spherical character of events vanishes close to the interaction point due to non perfect track extrapolations down to the center and due to possible secondary interactions. As a consequence, the angles under which the track elements are seen from a vertex may vary considerably so that angular projections - including ρ'/Z - give pictures which are very difficult to interpret. A way out are conventional cartesian projections with varying view points.

On the other hand, analysis gets more simple, as sufficiently close to the center no hits are visible and the reconstructed tracks can be approximated by straight lines.

In the following some methods are described for close inspection of the vertex region.

5.1 Smooth Standard Rotations

In order to find a good viewpoint for inspection of the interaction region smooth rotations are commonly applied. A rotation is characterized by the rotation axis, position of the viewpoint and angular speed.

The choice of these quantities is facilitated by taking into account the structure of the interaction and the feature one is interested in. Good choices for a rotation axis relative to the interaction are position and direction

- of a selected single track,
- of a reconstructed track leading to a secondary vertex,
- of the "jet axis" through the interaction point, i.e. the direction of flight of a group of particles.

A good choice for the axis relative to the display system is to position it into the screen plane. With a fixed rotation axis which is not interactively changed, different values of magnification may be applied for the direction parallel to the axis and perpendicular to it, so that angles appear enhanced. In figure 13a,b the corresponding ratio was set to a value of 4.

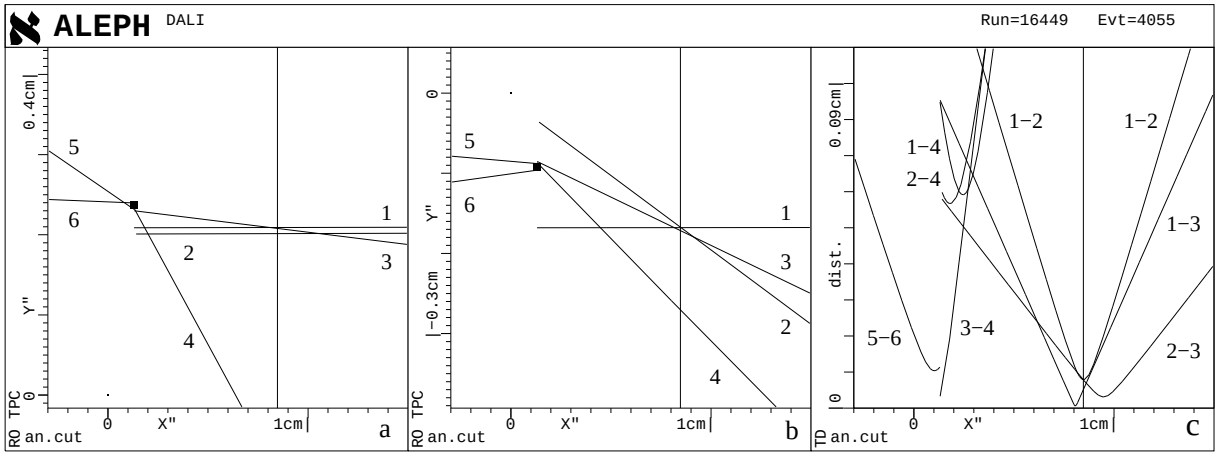

Figure 13: Crossing of tracks in space
a) tracks 1 and 2 parallel b) rotation around track 1 by 90° c)track pair distance

In order to determine the minimal distance between two tracks in space and to determine the points of nearest approach on the two tracks the following method can be applied:

1) select one of the two tracks as axis to lie in the screen plane (figure 13a track 1);

2) rotate around it until both tracks appear parallel in the projection (tracks 1 and 2 in figure 13a). Now the visible distance between the two tracks is equal to the distance of nearest approach of the two tracks in space.

3) rotate by 90 degrees. Now the points of nearest approach on the two tracks fall onto the visible crossing point of the tracks in the projection (figure 13b).

The method above is best understood by using a real mock-up of the problem. There seems to be no clear method for the corresponding problem, if more than two tracks are involved, as can again be verified using a mock-up. The only way out consists in checking separately all combinations of two tracks.

5.2 Artificial Display Cube

If one rotates lines, which run out of the picture on at least one side, we do not have the impression of a 3D rotation. The lines move up and down like wind screen wipers and one does not realize that the space position of the lines relative to each other is fixed.

This problem may be overcome by adding an "artificial display cube", ADC, to the picture as seen in figure 14a. The ADC is defined such that its edges are not parallel to the rotation axis. Its size is selected to be as big as possible without that the corners of the cube leave the window during rotation around the axis. In the “frozen” picture of figure 14a the ADC is larger. The ADC is not modified when zooming the tracks. The tracks are clipped at the faces of the cube (figure 14a). During rotation of the tracks together with the cube one gets a good impression of the 3D character of the tracks. This impression is mainly due to the clipping of the tracks at the faces of the cube.

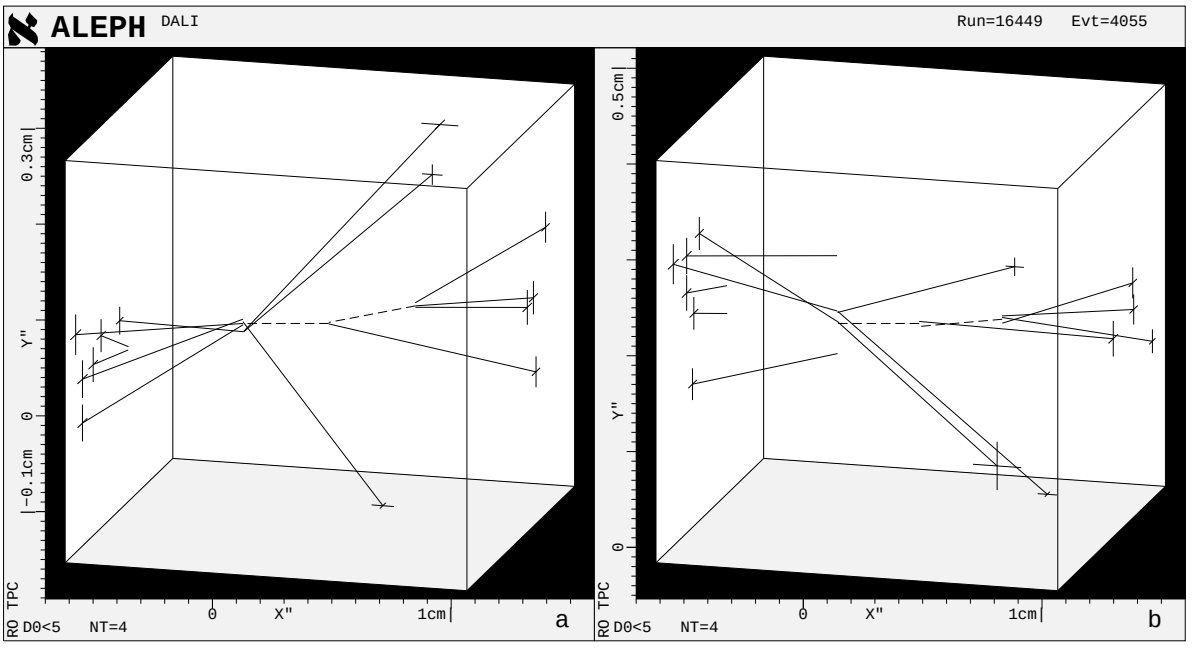

Figure 14: Artificial display cube

a) interaction near to the center b) same interaction rotated by 90°

Without rotation the space position of an exit point is ambiguous for the observer, i.e. it may either lie on one of the three front planes or one of the three back planes. This ambiguity is resolved by drawing crosses at each exit point, with their arms parallel to the edges of the corresponding face and their size being smaller for larger depth of the exit point. During rotation

the flagging of the endpoints by the crosses further helps the visualisation of the three dimensional structure of the interaction.

The ADC can be larger, when the rotation axis is tilted relative to the plane of the screen, which can however not be done, if the exact position of the points of nearest approach of two tracks is visualised as described in the previous chapter.

In order to find an optimal frozen picture for presentation purposes, two different procedures are helpful:

- The interaction is rotated until an optimal presentation is reached. Then the ADC alone is rotated with continuous clipping of tracks and maximizing the cube size until the whole picture appears optimal.
- An optimal presentation of the ADC is chosen. Then, the tracks alone are rotated with continuous clipping of the tracks until the whole picture appears optimal.

Whereas 3D continuous rotations may be helpful for analysis, it is difficult to present such continuous rotations to a larger audience. The presentation of a frozen picture as in figure 14a may be misleading, as it suggests to the audience a certain interpretation of the picture, namely that tracks which touch on the picture do touch in space. This may not be true, as can be seen from figure 14b. Whereas the positions of the crosses are three dimensional, the depth of the inner track points cannot be estimated, i.e. their position remains two dimensional (see chapter 4.1).

The clipping of tracks at the sides of the ADC and the elimination of tracks outside of the ADC are not only helpful to improve the perception of a continuous rotation, but also improves stereo vision on an adequate display. The elimination of tracks outside of the ADC improves stereo perception.

5.3 Display of the Track to Track Distance

By use of continuous rotations or by fixed projections seen from well chosen viewpoints, it is simple to identify groups of tracks, which do NOT cross. But the contrary is not true, i.e. one cannot easily verify if several tracks come close to each other in a small volume.

A method to overcome the latter problem consists in displaying the space distance between pairs of tracks via the following procedure (example: see figure 13a,b):

1) choose axis relative to the interaction as described in chapter 5.1 (track 1)
2) combine pairs of forward tracks (1-2,1-3,1-4,2-3,2-4,3-4) and backward tracks separately (5-6)
3) calculate the distance between the track pairs in a plane perpendicular to the axis;
4) plot this distance versus the position of the plane on the axis, down to the interaction point (see figure 13c).

The tracks 1, 2 and 3 are candidates for tracks originating from a secondary vertex, since the corresponding track pair distances have a very low minimum at $x = 0.85cm$ (figure 13c). This picture differs from all others in this paper as it combines tracks to pairs of tracks, whereas until now hits or tracks were drawn independently of the position of the other hits or tracks.

A vertical line was moved interactively to the crossing point of the projections of track 1 and 2 in figure 13b. The same line is then displayed in figure 13a and c to show the equivalence of the two methods applied.

6 The V-Plot, a Three Dimensional Representation for Visual Analysis of Tracks

It is the advantage of conventional projections, that they can be applied to a large variety of objects and experimental setups. However, this is also their biggest disadvantage, as it is difficult to optimize them for special problems. In the following we propose projections, which were specially developed for the ALEPH experiment. We will discuss a picture called V-Plot, which was developed for helices, i.e tracks of particles moving in a homogeneous solenoidal field. We will then generalize the underlying principles and apply them to a different experimental configuration.

6.1 The Helix Representation via the V-Plot

It was shown in chapter 3.3 and figure 8d that tracks are better recognized in a compressed φ/ρ projection than in *Y/X*. This is shown again in color plates 10a,b. The compression facilitates the identification of tracks, but not their separation, as the total picture space is reduced as well (color plate 10b). The best track separation is obtained via φ/ϑ (color plate 10c). As discussed before, a representation in φ/ϑ does not allow to estimate charge and momentum, in contrast to φ/ρ, and it is not possible to verify, if tracks really enter and leave the chamber.

Therefore it is tempting to use a linear combination of the two projections, namely $\varphi/(\vartheta + k\rho)$. In color plate 10d, a slightly modified projection $\varphi/(\vartheta + kD)$ is shown with $D = \rho_{MAX} - \rho$, where ρ_{MAX} is the outer radius of the tracking device, here the TPC. The value of *k* is interactively chosen and scales the gradient of the straight track images. This projection conserves most of the good features of both projections, namely approximately straight track images, the ease of momentum and charge estimation as in φ/ρ and the good track separation as in φ/ϑ.

φ/ρ and φ/ϑ are two projections, which together represent the full 3D information of the data. They may be replaced by the two symmetric projections, $\varphi/(\vartheta + kD)$, introduced above, and $\varphi/(\vartheta - kD)$. If $k > 0$, they represent the full 3D information as well (see color plates 10e,f). As last step, the two projections are drawn on top of each other as seen in color plate 10g. The two superimposed track images of a single track form a V pattern, where the exit point, $D = 0$, lies at the tip of the V.

A somewhat modified definition of the variable *D* is more useful: $D = R_{MAX}(\vartheta) - R$, where *R* is the spherical radius defined above and R_{MAX} the distance of the outer surface of the tracking detector from the center in the direction of the hit, so D is the distance from the hit to the outer surface of the TPC in this direction. If the tracking detector is of cylindrical form, R_{MAX} depends only on ϑ, i.e. $R_{MAX} = Min\left(\frac{\rho_{MAX}}{\sin\vartheta}, \frac{Z_{MAX}}{|\cos\vartheta|}\right)$, where the outer cylinder surface is given by ρ_{MAX} and $\pm Z_{MAX}$.

The interpretation of this so called "V-Plot", as can be derived from the equations (3) in chapter 3.2, is summarized in the following:

- V-position : ϕ, ϑ = *spatial track direction*.
- V-direction : *up or down* $\Rightarrow$ *particle charge*.
  (e.g. ALEPH: *up* $\Rightarrow$ *negative*, *down* $\Rightarrow$ *postive charge*)
- V-angle : $gradient \sim \frac{1}{P} =$ *particle momentum*$^{-1}$
  wide V's = high momentum,
  narrow V's = low momentum.
- V-width : proportional to *D*, i.e. to track distance from exit.
  The tip of the V denotes the track exit.
- curved V-arms : the track has either low momentum or its origin is outside the center.

This means, that one can retrieve the full 3D information from the V-Plot. This is due to the fact, that two projections are superimposed. As the ordinate φ is the same for the two projections, a hit is represented by two points, which may be replaced by a horizontal line connecting them. Such lines have three degrees of freedom. Their center point gives φ and ϑ and their length is a measure of the distance of the hit from the outer surface of the detector, so that one could in principle recalculate the three original hit coordinates. The V-Plot is therefore an abstract 3D representation of the TPC hits.

The V-Plot has a particularly high information content. However, one has to prove, that a human operator sitting in front of a terminal is able to work with these pictures, and especially, that the doubling of hits and of tracks does not give pictures, which are too complicated for visual analysis. Such an investigation cannot be done by theoretical arguments but by applying this technique to typical and to difficult events.

6.2 Application of the V-Plot, Example 1

To illustrate how to work with the V-Plot in practice, *Y/X*, φ/ρ and the *V*-Plot are compared in color plate 11 showing an event, which was cleaned by eliminating all noise hits, i.e. hits, which were not associated to tracks by the pattern recognition program. When stepping clockwise, i.e. with increasing φ, through the tracks, one can compare the track representations in *Y/X* (color plate 11a) with those in the V-Plot (color plate 11b). This comparison is simplified by passing through the compressed φ/ρ projection in color plate 11c.

On color plate 11 several tracks are labelled by their measured momentum in [GeV/c] to demonstrate the relation between momentum and V-angle and to help the reader to associate the track images in the different windows.

Some special tracks are blown up in the inserts of color plate 11. The region around the track labelled "kink", is blown up from the V-Plot (color plate 11h) and from *Y/X* (color plate 11e). The kink is very pronounced in the V-Plot when compared to *Y/X*. As this kink is mainly due to a variation of ϑ, it would be better visible in ρ'/Z, which is not shown here.

The V-arms of the blue track in insert (color plate 11h) and the V-arms of the yellow track in color plate 11b are curved indicating that the tracks do not originate from the center.

The red V of the 1.5 GeV/c track is blown up in insert (g). The scattering of the points around a straight line is due to the limited precision of the measurements and multiple

scattering. This demonstrates that one reaches a magnification, where the detector precision gets visible, so that one is neither limited by screen resolution nor by the human visual system.

The region around the 3.7 and 8 GeV/c tracks (red and blue in color plate 11b) is blown up as *Y/X* (color plate 11d) and V-Plot (color plate 11f). The two tracks have one point in common, hence the two tracks cross in space, which cannot be unambiguously derived from *Y/X*, as the depth of the hits is not represented. Many tracks crossing each other are found in *Y/X* (color plate 11a) but from the V-Plot (color plate 11b) one can derive, that no other tracks cross in space.

6.3 Application of the V-Plot, Example 2

A minor but rather helpful detail needs to be mentioned before discussing the next example. As $\vartheta = \operatorname{atan}\frac{\rho}{Z}$ increases with decreasing Z for a fixed value of ρ, left and right would be inverted when comparing φ/ϑ with ρ'/Z. To avoid this, the ϑ-axis is defined as pointing to the left in the V-Plot and in all φ/ϑ projections. This is indicated in figure 15a by the arrows.

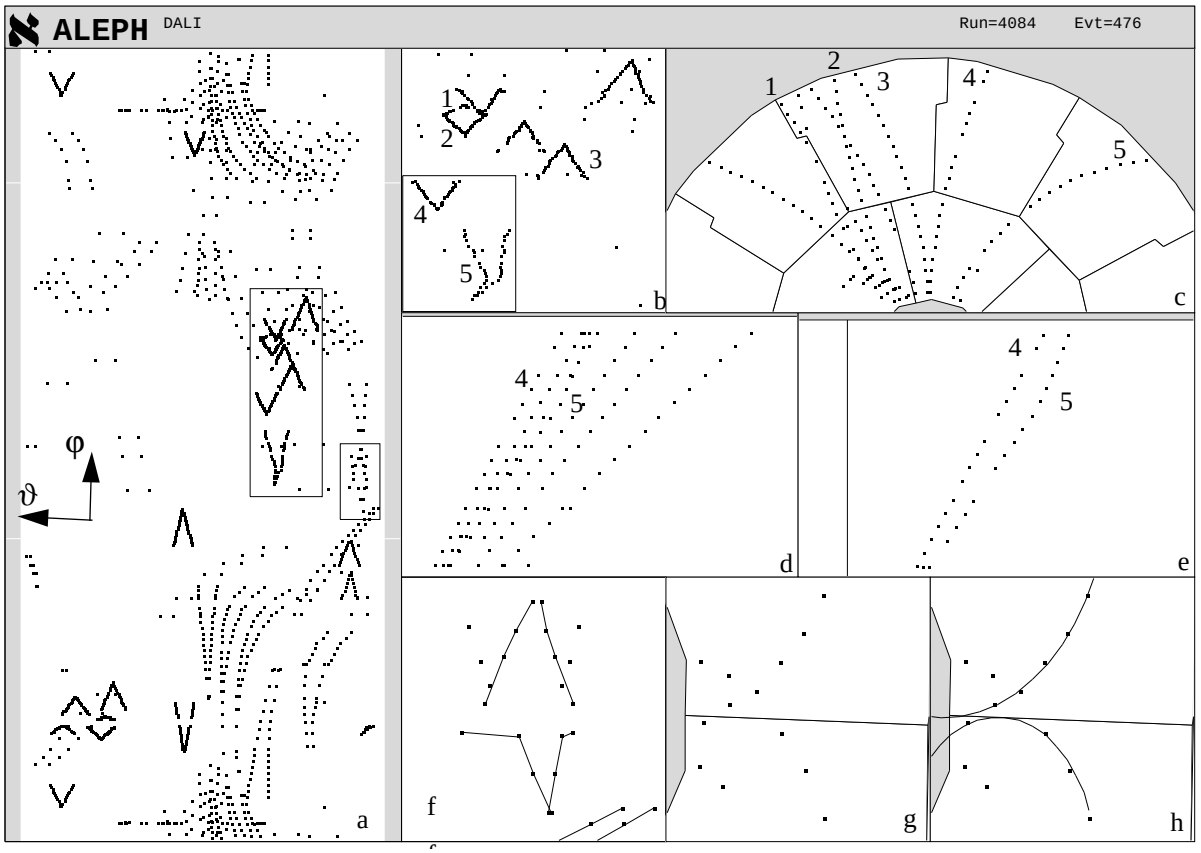

Figure 15: Use of the V-Plot

a) V-Plot
b) section of the V-Plot
c) *Y/X*
d) ρ'/Z
e) ρ'/Z cleaned
f) section of V-Plot with connected hits
g) *Y/X*
h) *Y/X* with hits and tracks

Figure 15a shows the measured hits (noise not removed) for a typical event of the ALEPH TPC as V-Plot. The V-Plot provides a simple tool to select hits or tracks through a volume

defined in position and size via φ, ϑ and ρ. This volume can subsequently be visualized in other projections[14] or again as V-Plot, as is shown in the following examples:

- The angular section defined by the large rectangle (15a) is shown as V-Plot in 15b, as *Y/X* in 15c and as ρ'/Z in 15d,
- the angular section defined by the small rectangle in 15a is shown blown up in 15f and as *Y/X* in 15g,h,
- from the tracks seen in figure 15b, two are selected through the rectangle in this figure and shown as ρ'/Z in 15e.

The kink in track 5, which is due to the decay of a charged particle, is enhanced through the vertical compression of the V-Plot (15b) as compared to the kink shown in ρ'/Z (15e).

The blow-up of the V-Plot (15b) shows a quadrilateral pattern typical for the decay of a neutral particle into a positive (2) and negative (1) particle. The corresponding tracks have a common origin in the TPC, i.e. away from the primary vertex. No other pattern of this form is found in 15a and 15b, i.e. no other decay of a neutral particle exists in the TPC. It is rather difficult to confirm that fact from *Y/X* and ρ'/Z.

The assignment of hits to tracks by the pattern recognition program, as indicated through the lines in 15f and 15h, looks rather likely in the V-Plot, where it is checked in 3D, compared to *Y/X*, where the depth information is lost (see also color plate 8c,d,e). The probably false association of the hits to tracks by the program may be due to the fact that the two tracks cross in space, as can be seen from 15f.

6.4 Extrapolation of Tracks via the V-Plot

In chapter 3.7 the φ/ϑ representation of calorimeter cells was discussed. However no satisfactory method was found to associate the tracking data from the TPC to the calorimeter data (see figure 10d). This problem is solved by use of the V-Plot.

Figures 16a and 16b show the front and side view of two tracks and those calorimeter hits, which lie in the same direction. (The same event is used as in figure 10). The φ/ϑ projection of the three layers of active calorimeter cells is shown in figures 16d,e,f, where the shower development can be estimated easily, as discussed before. In figure 16c the V-Plot of the two tracks is superimposed to the calorimeter islands, so that the clusters created by the two charged tracks can be identified. If for one reason or the other the last hits of a track are missing (which is not the case here), the exit position of the track can easily be deduced, i.e. even in this case tracks and showers can be correlated.

As seen in this example, the V-Plot is that representation of tracking data which is complementary to the most used display of calorimeter data, namely the Lego Plot.

The V-Plot is also applicable to backward extrapolations of tracks into inner tracking subdetectors, e.g. into a vertex detector, as long as three dimensional data are recorded or in the case that the hits are confined to few layers, which are separately investigated. In the latter case, the variable D defined in chapter 6.1 should be redefined such that the tip of the V points to the selected layer. However, backward extrapolation further downwards via the V-Plot may lead to very complicated pictures, when getting too close to the vertex. This is the case if tracks do not point precisely to the vertex due to measuring errors, secondary decays etc., so that the variation of φ and ϑ gets very large.

[14]The angles are interactively defined by use of a rubber band cursor, the vales of ρ is preset.

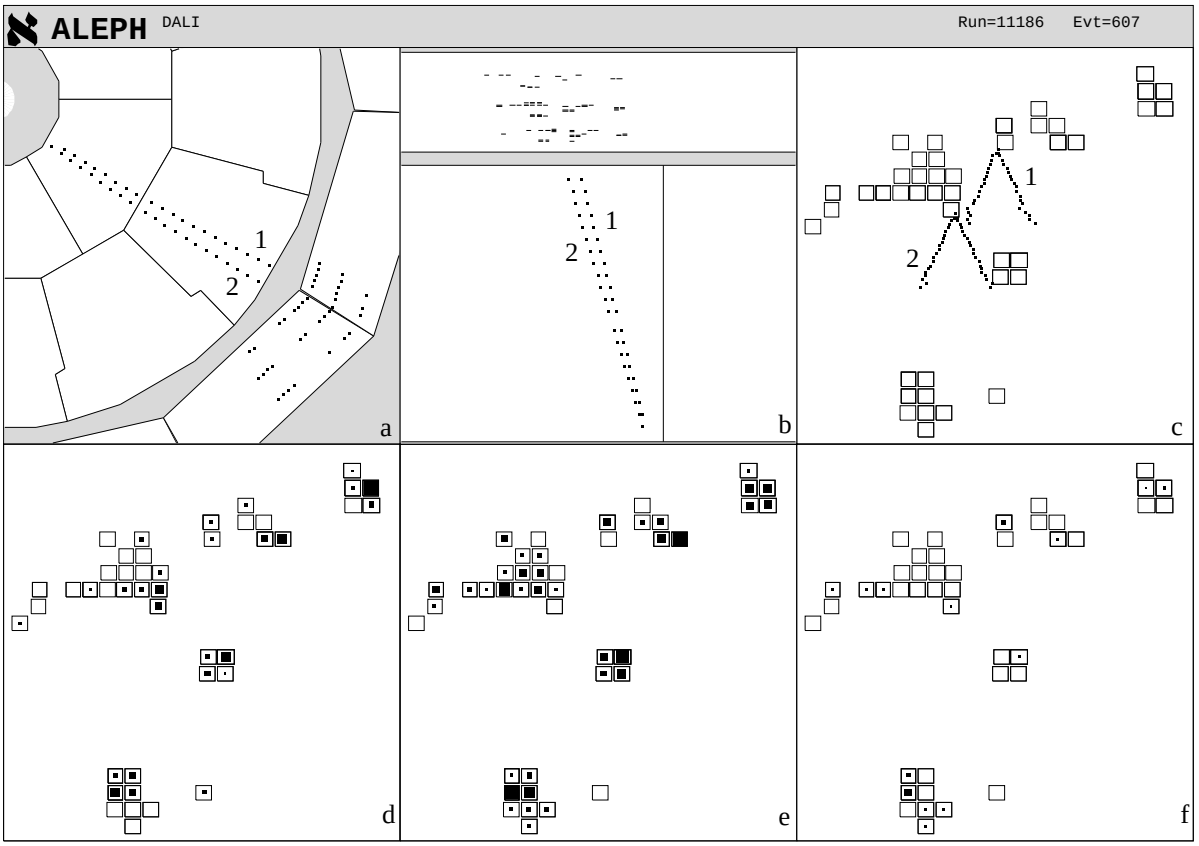

Figure 16: Association of TPC tracks to a calorimeter (The area of the squares is proportional to the deposited energy).

a) *Y/X* b) ρ'/Z c) V-Plot + calorimeter islands

d) φ/ϑ of calorimeter layer 1 e) φ/ϑ of calorimeter layer 2 f) φ/ϑ of calorimeter layer 3

6.5 The V-Plot for Super High Multiplicity Events

Figure 17a shows the front view, *Y/X*, for a simulated "super event" with 221 tracks. The simulation was accomplished by superimposing many events from the ALEPH TPC. Only few tracks can be partly identified in the front view even when blown up (see figure 17b). The display of such "super events" in other conventional projections yields even more difficult pictures due to cycloidal track patterns. The simultaneous use of two conventional 2D projections, in order to examine the tracks from several sides, excludes itself, as it is practically impossible to correlate the tracks. These projections can only be used, if one succeeds to apply cuts so that sufficiently few tracks are displayed.

Track identification is possible via the V-Plot (figure 18a), as long as the tracks leave the chamber, i.e. do not spiral. By blowing up crowded regions (the framed region in 18a is blown up in 18b) practically all non spiralling tracks can be identified.

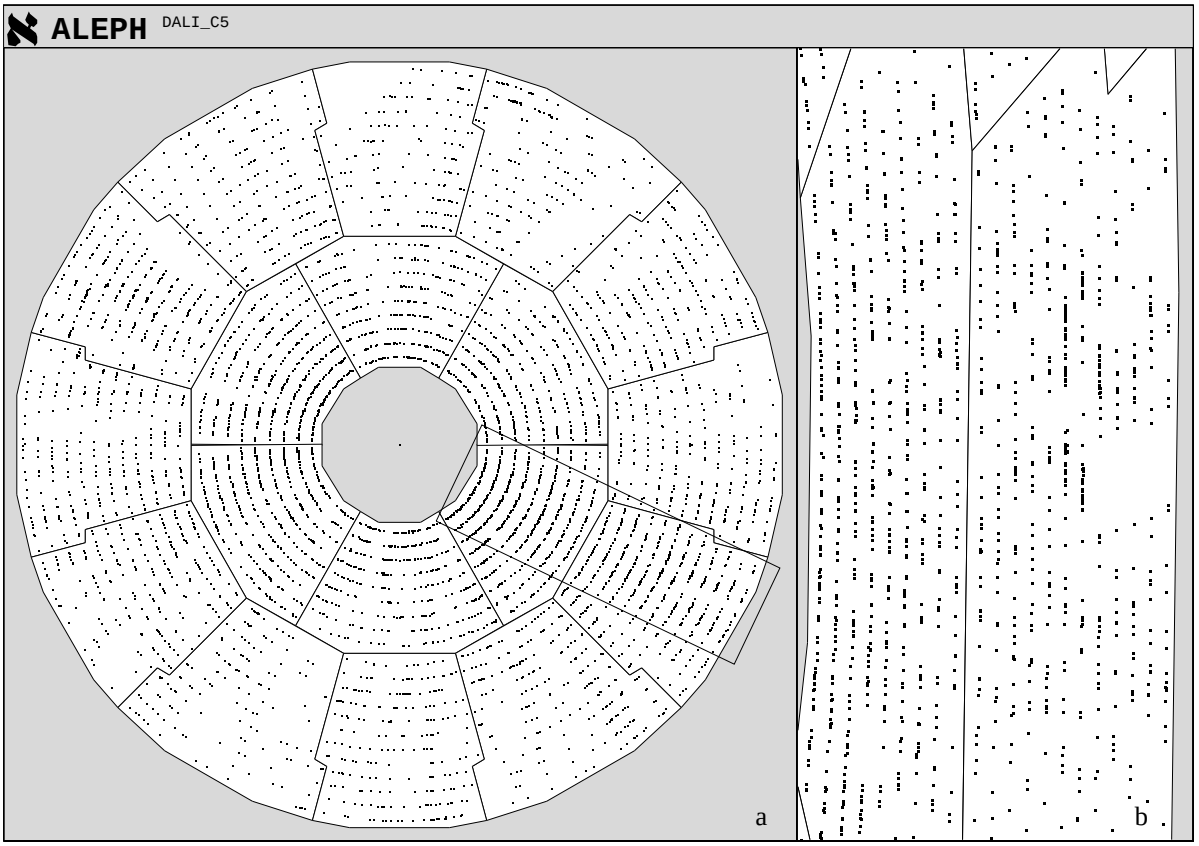

Figure 17: Super high multiplicity event with 210 tracks

a) *Y/X* b) blow-up of Y/X defined by the rectangle in figure a

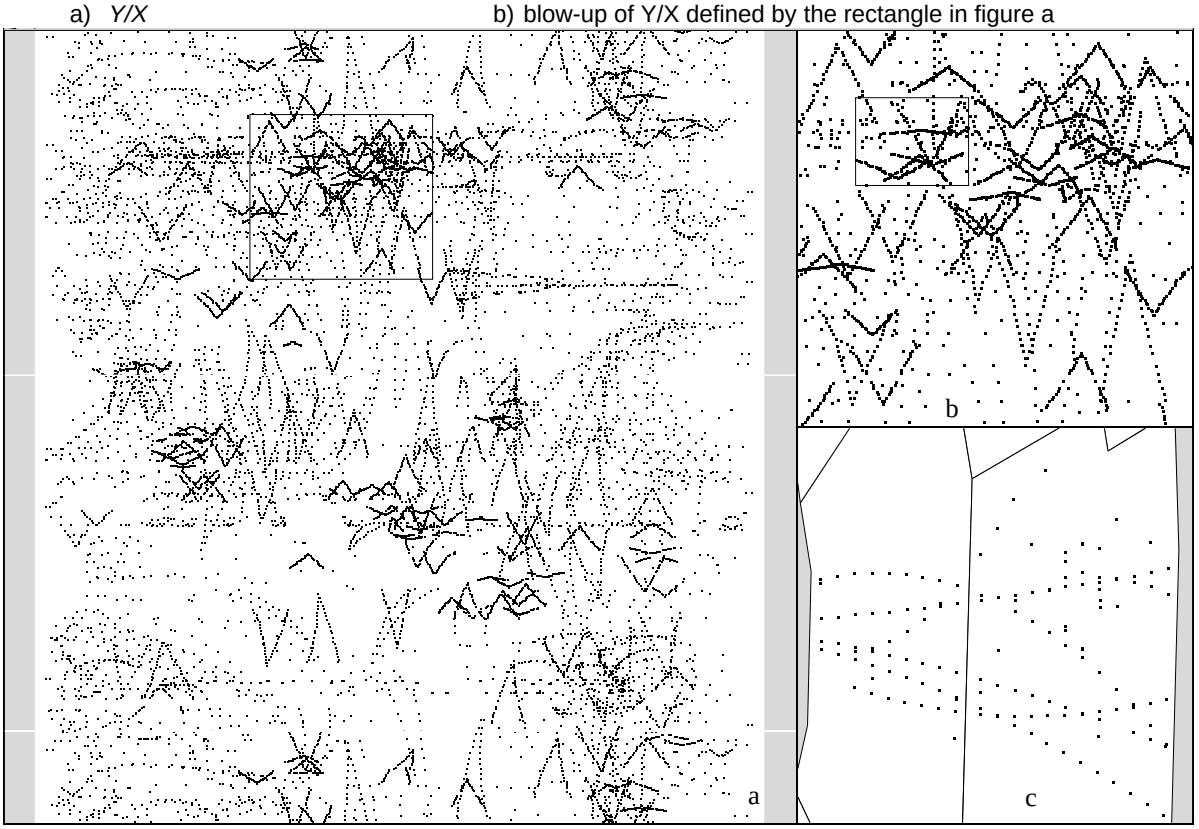

Figure 18: Super high multiplicity event with 210 tracks

a) V-Plot b) blow-up of the V-Plot c) *Y/X* of the hits selected through the rectangle of figure b.

By defining a volume through an angular section, as discussed in chapter 6.3, single tracks or groups of tracks can be selected and displayed in conventional projections. The hits contained in the rectangle of figure 18b are shown in *Y/X* in figure 18c, where tracks are easily recognized. This track selection acts like a depth cut (ϑ-cut, not Z-cut!) on *Y/X*. Despite the high multiplicity of such events it may be possible to generate conventional pictures suitable for talks and papers by applying selections of this type.

6.6 Generalisation of the V-Plot

The V-Plot technique is constrained to 3D data only, which might either consist of 3D hits or of 3D track segments. In the latter case the spatial position may be measured directly or may be determined through the averaging of sets of hits or may be obtained through other methods.

From the special form of the V-Plot, described above, we will try to deduce general rules to construct a V-Plot, namely:

- The V-Plot is a superposition of two symmetric projections. For each 3D hit two points are drawn. The position of the center between them and their distance *kD* are calculated from the coordinates of the hits. The angle β under which the two points are drawn can be chosen in a convenient way. It is important that no other information than the 3D position of the hit is used. Especially, the association of a hit to a track is not taken into account.
- The projections must be chosen in a way to (approximately) linearize tracks and to compress all of them simultaneously. An optimal compression is achieved, if for *k=0* a radial straight track is seen as a single point.
- The distance *kD* between the two point images is a measure for the distance *R* of the 3D hit from the center.
- H,V and *D* should be chosen in such a way that charge and momentum can be estimated.

If a variable U (or a function of variables) is (approximately) constant for all points of a track, then *H,V,D* and β may subsequently be modified through this variable in order to fulfil the above requirements and to yield a usable picture, e.g. H may be changed to $H' = H \cdot F(U)$. Under this transformation straight V-arms remain approximately straight.

Various realizations of V-Plots are published elsewhere [5]. In the next chapter one of them is presented.

6.7 The V-Plot for Straight Track Sections Outside a Magnetic Field. (TPC Tracks of the NA35 Experiment)

In the fixed-target heavy-ion experiment - NA35 - at the SPS/CERN a large number of particles leaves the target in very forward direction, defined as *X*-direction [6]. A perpendicular homogeneous magnetic field (in *Z*-direction) bends the particle trajectories in the *X*-*Y* plane. About six meters downstream, outside the magnetic field, straight track segments are recorded by a TPC, delivering 3D track hits. Figure 19a shows the setup in Y/X, with the vertex at the very left and a rectangular block of the TPC hits at the right. A blow-up of the hits is shown in figure 19d and the other two projections *Y/Z* and *Z/X* in figures 19b,c respectively. The only projection, where tracks can be distinguished, is *Y/Z*. However, it is difficult, if not impossible, to estimate charge and momentum.

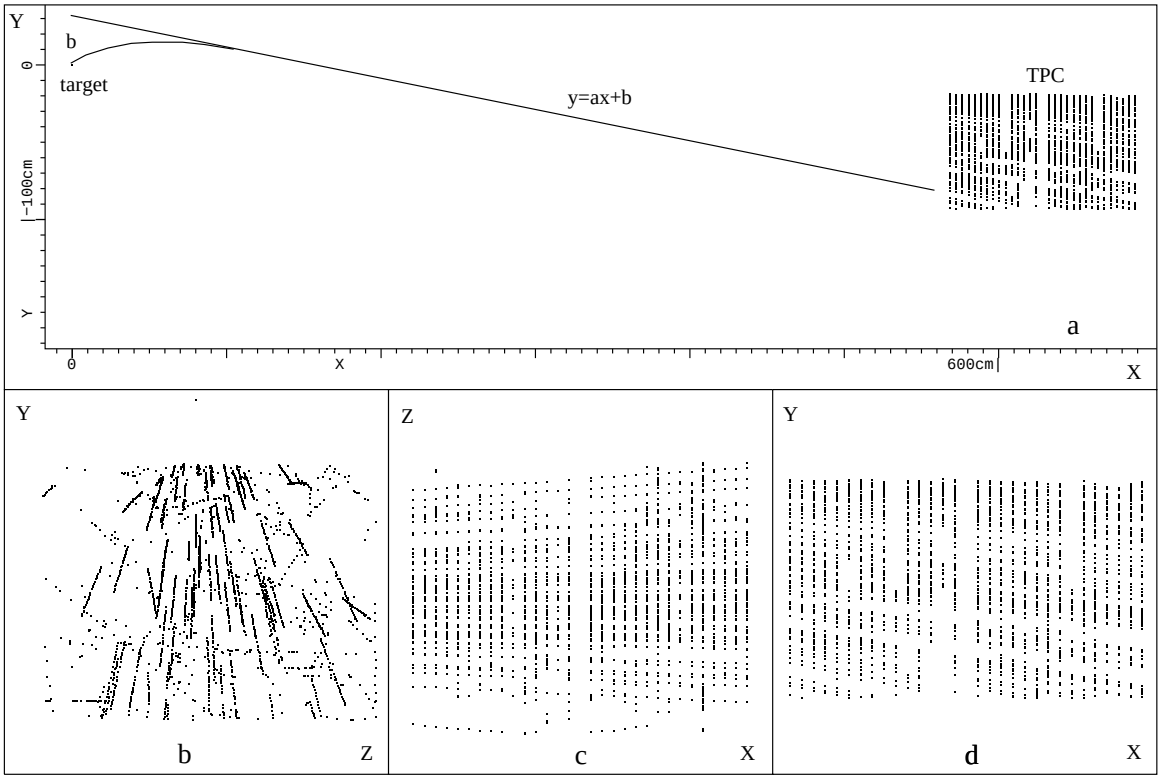

Figure 19: An event from the NA35 TPC

a) setup of the experiment in *Y/X*
b) *Y/Z* c) *Z/X* d) *Y/X*

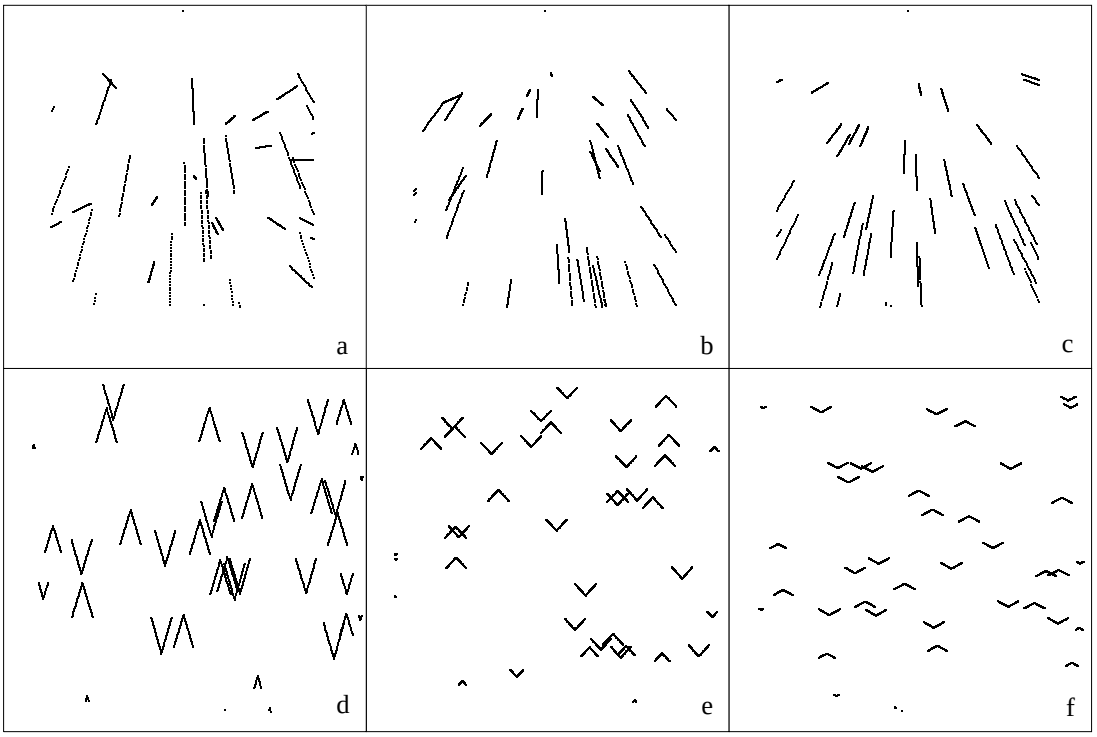

Figure 20: Simulated hits of tracks with predefined momenta P (without measuring errors)

a) *P=2 GeV/c*, *Y/Z* b) *P=6 GeV/c*, *Y/Z* c) *P=12 GeV/c*, *Y/Z*
d) *P=2 GeV/c*, *V*-Plot e) *P=6 GeV/c*, *V*-Plot f) *P=12 GeV/c*, *V*-Plot

The straight tracks in the TPC can be described by $Y = aX + b$ and $Z = cX$, where the gradient a depends on the direction and the momentum of the track; the offset b is an approximate measure of the track momentum, hence is of higher interest.

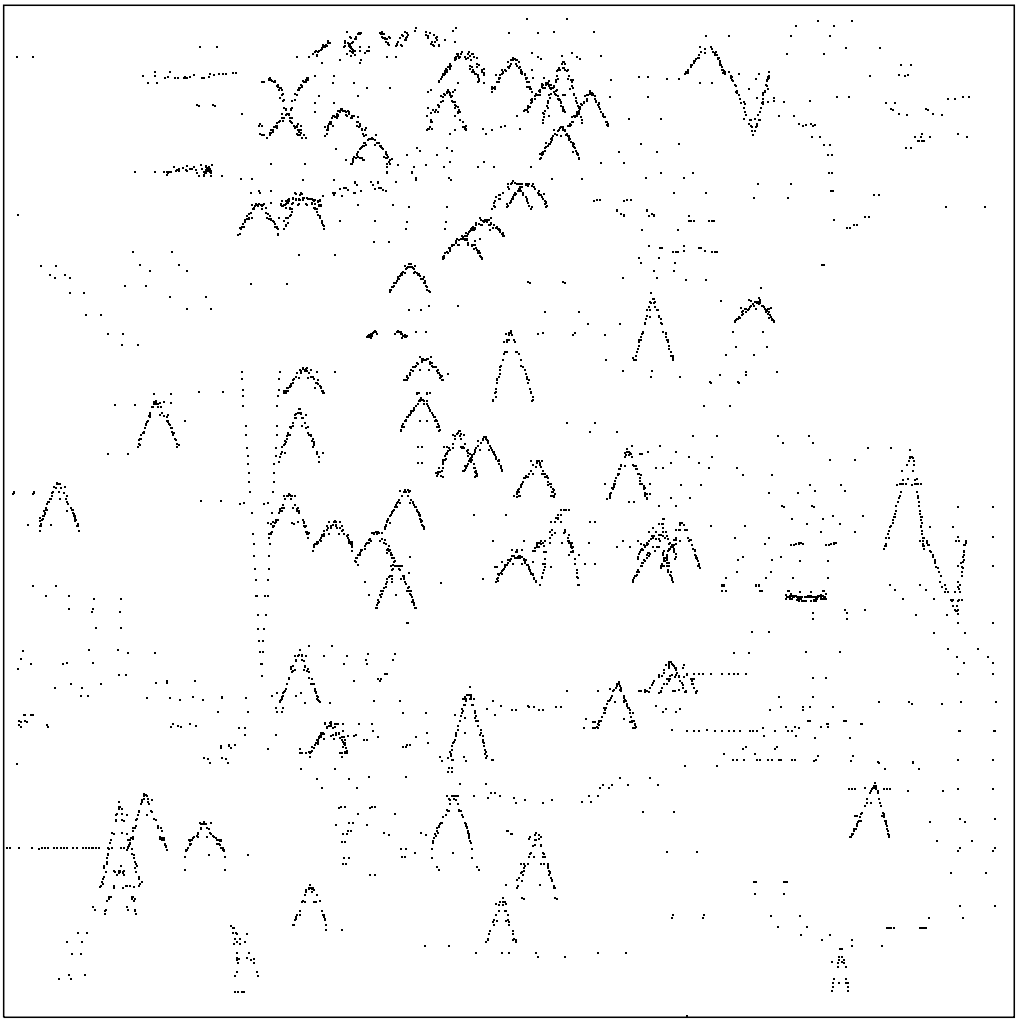

Figure 21: V-Plot of the same NA35 event as in figure 19

The general V-Plot rules of the previous chapter are fulfilled by setting $H = \frac{Z}{X}$, $V = \frac{Y}{X}$, $D = X_1 X_2 \left(\frac{1}{X_1} - \frac{1}{X} \right) \approx X - X_1$, where X_1 and X_2 define the position of the entry and the exit plane of the TPC, respectively. Then one displays V versus $H \pm kD$.

If $k=0$, this V-Plot is identical to $\frac{Y}{X} / \frac{Z}{X}$, which is rather similar to the best of the above projections, namely *Y/Z* (figure 19b); the interpretation of the V-position is therefore straightforward. In $\frac{Y}{X} / \frac{Z}{X}$ the image of a radial straight tracks ($b = 0$) is reduced to one point. For $k \neq 0$ the V-arms are drawn in the symmetric projections $V / (H+kD/2)$ and $V / (H-kD/2)$. For the points of a single track ($\frac{Z}{X} = c$) these projections are identical to $\frac{Y}{X} / \frac{1}{X}$ apart from a linear transformation. As discussed already in chapter 3.6, straight tracks transform into straight tracks

in this projection, as $\frac{Y}{X} = a + b\frac{1}{X}$. Therefore the arms of the V are straight, their gradient *b* is a measure of the particle momentum and the V-direction gives its charge, so that one gets the same features as for the V-Plot of the ALEPH TPC. One feature is especially important, namely that both, momentum and charge, can be estimated locally from the display of the TPC hits only without displaying the vertex point.

Figure 20 shows a simulation of track hits with either 2, 6 or 12 GeV/c in *Y/Z* and as V-Plot. It is evident, that the shape of the track images, the V's, depends only on momentum and not on the position of the tracks.

The NA35 event shown before in figure 19 is displayed in figure 21 as a V-Plot, on which the tracks are easily identified, and from which one can extract momentum and charge of the particles[15]

6.8 Interactive Correlation of Different Windows

It is often convenient to work on several windows synchronously

- with the same projection but different magnifications,
- with different projections,
- with the same projection and magnification but different data.

The following problems may arise:

- Identify the same object on the same window, if the object is large or is drawn several times.
- Identify the same object on different windows
- Identify the same 3D position in different windows.

Correlation of objects may be done either through

- colors (chapter 2.4) or
- "pick and move"
- "pick and blinking" or highlighting.

The pick and move method works as follows:

1) an object is identified by picking on a selected window.
2) the pointer is moved interactively to a different position or window,
3) the pointer is moved by program to the closest occurrence of the previously identified object.

Instead of moving the pointer to the previously identified object, the object itself may be blinked or highlighted on all projections.[16]

To identify a position on different windows with different projections one calculates the projections of an artificial 3D point on all windows and draws corresponding pointers at these positions. Via the mouse a selected pointer can be moved, so that the coordinates of the virtual point are modified. The pointer positions in the other views move accordingly. This method is most effective, if one of the projections is the V-plot, as most tracks can be identified through their direction.

---

[15]The data originate from one of the very first events ever recorded in the NA35 TPC, which was not yet well aligned.

[16]This method is not applied in DALI.

7 The Puzzle-Plot, a Three Dimensional Representation of Calorimeter Data

Figures 16d, e, f show three layers of a calorimeter side by side, so that one can follow the shower development by comparing the three pictures, as discussed before. It is possible to recognize, which cells in the different layers form a cluster, i.e. belong to the same shower. Thereby it is possible to verify independently the clustering algorithm of the pattern recognition program. With increasing number of layers, however, this gets more and more tedious.

An example of a calorimeter with a large number of layers is the ALEPH Silicon Calorimeter, SICAL. It has a cylindrical structure and consists of two parts 2.5 m down and upstream from the interaction point with a length of 12 cm, an inner radius of 6 cm and an outer one of 14.5 cm. Each cylinder is divided into 12 disks, each disk is divided into 16 rings and each ring into 32 angular sections with $\Delta\varphi = 360^\circ / 32 = 11.25^\circ$. Thus the detector consists of 6144 cells in 12 axial and 16 radial layers. Each of the disks is rotated by $\Delta\varphi / 3$ with respect to the previous one, i.e. the disks are “staggered”.

In color plate 12a all active cells are displayed in the wire frame technique in a perspective view. A section is blown up in color plate 12b. All blue cells are considered by the clustering algorithm to belong to the same cluster. The same is true for the pink cells. The yellow cells do not touch these two clusters and have too little energy to form a cluster by themselves, i.e. they are regarded as noise by the clustering algorithm.

However, the picture is very complicated due to the large number of active cells and due to the fact, that perspective drawings are less well comprehensible if lines are curved and the objects have different orientations. The picture would get even more complicated if in addition one would try to display the amount of energy deposited in the active cells.

By use of such pictures it is possible to prove, that clusters do not touch each other, if at least one suitable viewing direction can be found, where they appear separated (see the blue and pink clusters in color plate 12). It is more tedious to prove that all noise cells (yellow) are not connected to one of the clusters, as it may be necessary for this purpose to select a different direction of view in each case. For complex clusters, however, it is impossible to identify visually all cells belonging together. The Puzzle-Plot, explained below, offers a way out. However, it is not intuitively understandable.

The rules to interpret the Puzzle Plot are best explained by ignoring for a moment, what is known about the calorimeter. Color plate 13a shows a Puzzle Plot and color plate 13b the blow-up of a section. The blow-up shows 10 black fields separated by white lines, where each field contains one or several “triple crosses”. A triple cross is composed of one vertical bar and three equidistant horizontal bars of identical color. The yellow one in color plate 13b may serve as an example. The crossing points of the bars lie along three diagonal black lines and are emphasized by a black spacing between the bars. These lines become clearly visible if there is more than one triple cross in one field.

Next we define the connection between all connected triple crosses applying the following rules:

Triple crosses in neighbouring fields are connected if:

1) one (or two) of their horizontal bars touch each other, or
2) their vertical bars touch each other.

Triple crosses in the same field are connected, if

3) their vertical and horizontal bars have minimum distance between each other, which in this example is equal to the distance of the pink bars in one field.

Triple crosses in non neighbouring fields are connected, if there is a path of connected neighbouring triple crosses between them, applying the rules given above. One sees clearly, that all blue triple-crosses in color plate 13b are connected directly or indirectly via other triple crosses. The same is true for the pink ones, whereas the yellow one is unconnected.

There is a close correspondence between these rules and the problem to find clusters in the SICAL, as the black fields are a mapping of the towers arranged vertical to the Z-axis and the triple crosses describe the position of the active calorimeter cells. The position of a triple-cross is defined by three independent variables. Two (*H,V*) define the position of the field in which it is drawn, and one (*D*) defines the position of the triple-cross inside the field along the diagonal lines. The position of a cell in the SICAL is defined by φ, Z and ρ. If one sets $V = \varphi$, $H = Z$ and $D = \rho$, the calorimeter is mapped onto the Puzzle-Plot, so that it is possible to visualize the cells in all three dimensions. This allows to check the association of cells to clusters.

The arrangements of the fields reflects the staggering, which necessitates the use of three horizontal bars in order to visualize the connection in Z-direction (rule 1 above).

One notices from color plate 13a, that in the fields denoted by a ' * ', triple crosses exist, which cannot be connected to the blue cluster, directly or indirectly. This is due to the fact, that the real clustering algorithm of the ALEPH SICAL allows the connection of cells, if they touch at a border lines parallel to the Z-axis, i.e. triple crosses in neighbouring fields above or below are connected if:

4) their vertical lines are displaced by one step.

The application of this rule is easy in the puzzle plot, but very difficult in the wire frame representation.

The special form of the Puzzle-Plot as described above may of course vary with the structure of the calorimeter displayed. The triple-crosses can be regarded as symbols displaying the depth of the cell. There may be other symbols useful for this purpose.

The representation of the SICAL data via the Puzzle-Plot allows in a simple way to represent in addition the energy deposit in the active cells. At the center of the three horizontal lines of a triple-cross a horizontal line of a different color (red and white in our example) is drawn, the length of which is proportional to the deposited energy. Thus one gets the visualization of a three dimensional scalar field.

8 Classification of Pictures

The pictures discussed in this paper may be grouped into three classes:

1) realistic pictures:

   They are obtained by either a sequence of rotation, linear scaling and projection or by central perspective, in both cases cutting away parts of the detector, if useful. The resulting pictures are intuitively understood.

2) schematic projections

   They comprise

   - all other linear transformations, e.g. a change of aspect ratio.
   - the Y/X projection with fish-eye.
   - the ρ'/Z projection with or without fish-eye.

   In many cases schematic projections are better understood and easier to use than the realistic projections. The best known projection of this type from another field is the Mercator projection used in geography.

3) abstract pictures:

   They show no resemblance to the original objects. They comprise the angular projections φ/ρ, φ/z and φ/τ as well as the V-plot and the puzzle plot. They are not intuitively understandable and need training to be understood. Therefore, they are not suited for general presentations but they are usually very powerful.

Often only realistic pictures are implemented on high end graphics systems, such reducing their capabilities.

9 Conclusions

Visual representations are used for two different purposes, namely for

- presentations, i.e.talks and papers,
- visual analysis.

If pictures are used in presentations they should be intuitively understandable, without requiring long explanations. If a picture is not just used to catch the eye, the information the lecturer or writer wants to pass on to his audience must be comprehensible from the picture. This is even more demanding, if a picture is shown in a talk for a short time only. To this aim pictures must be sufficiently simple, still matching the complexity of detectors and events.

In the case of a cylindrical detector the best pictures are obtained using cross-sections, i.e.:

- ρ'/Z as side view and *Y/X* as front view, with the endcaps omitted in *Y/X*. If these projections are applied, the various subdetectors do not overlap, so that both hits and subdetectors can be drawn together and hits fall onto the image of the subdetector, by which they were recorded.

These images can be further improved by:

- applying (non linear) fish eye transformations, so that the inner chambers are enlarged and the outer ones reduced in size;
- displaying the energies deposited in the calorimeters as histograms in the form of structured areas;
- coloring the subdetectors;
- choosing suitable colors for hits and tracks. Tracks are better separated, if neighbouring ones are colored differently.

Three dimensional information can be transmitted by

- showing *Y/X* and ρ'/Z side by side. In this case color may be used to correlate objects in the different pictures.

These methods yield clear pictures in the case of experimental setups like the ALEPH detector. Furthermore, it is of big help to carefully select events, which show the required features, but which also give good pictures.

However, if events with very high multiplicities are to be shown, a display of the data may yield useless pictures, i.e. the limits of these methods may be met. A way out might be the application of one of the following methods, namely

- to draw the data in a simpler form, i.e. tracks (lines) instead of hits (points),
- to restrict the amount of displayed data by use of information given by the pattern recognition program, e.g. by a cut on track momentum,
- to display data from sufficiently small volumes, where the problem of how to find and define such a volume arises,
- to use non-conventional projections like the V-Plot or the Puzzle Plot, which yield clearer pictures. However, they have the big disadvantage, that the listener or the reader is required to have the necessary knowledge for their interpretation.

The above conclusions are also valid for the visual analysis of tracks, where it is often necessary to display the basic data, i.e. display the hits instead of tracks. It is normally not possible to restrict the analysis to specially selected, clear events.

Most events have a large amount of tracking information. Track recognition is drastically improved through the following concepts:

- Track compression, i.e. a low magnification in track direction and a large one perpendicular to it.
- Track Linearization, which facilitates compression, but also recognition and visual extrapolation of the tracks. In the case of helices this is achieved using angular projections.
- Use of projections which allow the local estimation of track features, e.g. particle charge and momentum.

Through the first two methods it is possible to increase the magnification of a track in its full length to a level, where the errors of data recording become apparent, i.e. the limits imposed by screen and eye resolution are overcome.

If three dimensional data are available, two further concepts get important, namely

- the use of orthogonal projections,
- the overlay of two projections to transfer 3D information.

A good realization of the above concepts is found in the V-Plot, the mathematical formulation of which depends on the experimental setup. Furthermore, the V-Plot is a powerful means to extrapolate tracks to calorimeter representations like the Lego Plot.

Whereas the limits of the conventional methods seem to be reached when examining difficult events, the limits of the V-Plot technique still seem to be further away. This technique is however constrained to real three dimensional data, i.e. 3D hits and 3D track segments.

Calorimeter data are best displayed as Lego Plot or through pictures with similar structure, e.g. φ/ϑ, but different energy representation. Different layers projected side by side allow to judge the shower development, where the island representation helps to associate the clusters in different layers.

The use of this technique, however, gets more and more tedious with increasing granularity of the calorimeter, i.e. if many layers exist. A way out is shown in the Puzzle Plot, although it may be limited due to screen and eye resolution.

In short, the aim of visual representations, namely to transfer data from the computer into the human brain, can still be accomplished in a fast, unambiguous and efficient way. Even for more complex detectors and events, display methods are available to present the full data. However, the price to be paid is the use of more abstract representations. If one is ready to accept this complication, visualization of events will continue to serve as a helpful tool for representation and analysis.

10 Acknowledgements

The successful construction and running of the ALEPH detector by the collaboration provided the events, for which the methods described in this paper were developed. During development of these techniques we have had input from many of our colleagues in ALEPH. We owe special thanks to Chris Grab, Salvador Orteu, Mark Parsons, Raimund Vogl, Gabi Waltermann and Rongfen Xu for their valuable contributions to the program and to Brigitte Bloch-Devaux, Jürgen Knobloch, Dieter Schlatter and Jack Steinberger for helpful discussions and suggestions. For information on NA35 we thank Ingo Schneider and the NA35 collaboration for providing us with data. For help with the program FrameMaker we acknowledge gratefully the help of Herbert Mettler and Mario Ruggier.

11 References

[1] H.Drevermann, D.Kuhn, B.S.Nilsson, 'Is there a Future for Event Display?', *Proc. of 1992 CERN School of Computing*, L'Aquila, Italy, CERN Yellow Report 93-03.
[2] D.Decamp et al., *Nucl.Instr.Meth.* A294 (1990) 121.
[3] H.Drevermann and W.Krischer, *Nucl.Instr.Meth.* A239 (1985) 160.
[4] This method was proposed by M.Mermikides.
[5] H.Drevermann, C.Grab and B.S.Nilsson, 'How to Represent Three Dimensional Data of Events from High Energy Physics?' *Proceedings of the international conference on Computing in High Energy Physics* 91,Tsukuba, Japan, page 545. Universal Academy Press, INC.-Tokyo.
[6] J.W.Harris et al., *Nucl.Instr.Meth.* A315 (1992) 33.
[7] D. Travis, *Effective Color Displays, Theory and Practice*, Academic Press 1991, p. 53, 116.
[8] ibidem, p 49.

12 Further Reading

[9] H.Drevermann and C.Grab, *Int. Jour. Mod. Phys*. C1 (1990) 147.
[10] H.Drevermann, C.Grab, D.Kuhn, B.S.Nilsson and R.K.Vogl: 'A New Concept for Visual Analysis of Three Dimensional Tracks', published in: *New Trends in Animation and Visualization*, edited by N.Magnenat Thalmann and D.Thalmann, John Wiley & Sons.